

2.4 Model Input Data and Sources

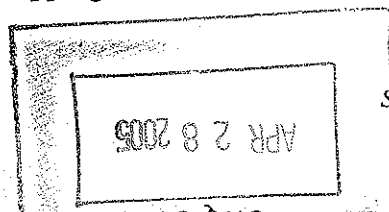
The following section contains the site location, local and regional subsurface geology, and the hydrologic and geologic parameters used to run the *DuPont Basic Plume*, *DuPont Multilayer Pressure*, *DuPont Multilayer Vertical Permeation*, *DuPont Molecular Diffusion* and *DuPont 10,000 Year Waste Plume Models* for the Lyondell Chemical Company, Channelview Plant. Source of each parameter is discussed and justified for use in the modeling.

2.4.1 Location

The Lyondell Chemical Company, Channelview Plant is located on the Quaternary Coastal Plain of Southeast Texas in the Peter J. Duncan Survey (A-232) and the B. Sessums Survey (A-733) in Harris County, Texas. Plant elevation is approximately 41 feet above mean sea level (MSL). Figure 1-1 shows the plant boundary and locations of the two injection wells and the topography of the area surrounding the Channelview Plant. Additional underground injection control facilities that may affect disposal at the Lyondell Chemical Company, Channelview Plant are the Equistar Plant Well 1 (WDW-36), the Merisol Plant Well 1 (WDW-147) and Plant Well 2 (WDW-319), the Atofina Plant Well 1 (WDW-122) and Plant Well 2 (WDW-230), the Vopak Plant Well 1 (WDW-157), the GNI Plant Well 1 (WDW-169) and Plant Well 2 (WDW-249), the Hampshire Plant Well 1 (WDW-222) and Plant Well 2 (WDW-223), and the Shell Plant Well 1 (WDW-172) and Plant Well 2 (WDW-173). The location of these wells in relation to the Lyondell Chemical Company, Plant Wells is shown in Figure 2-1. Additionally, Cobra Operating Texas Northern Railway #6 is a permitted Class II saltwater injection well, located in the 2.5-mile radius Area of Review. This well is currently completed in the lower Frio C Sand. Locations for the two Lyondell Chemical Company injection wells, the offset injection wells, and the artificial penetrations are digitized in local reference to the State of Texas X,Y coordinate system (units of feet). These coordinates are translated to model units by setting the model reference point ($X_{\text{model}}=0$, $Y_{\text{model}}=0$) to Texas State Plane Coordinate $X = 3,230,000$ and Texas Coordinate $Y=740,000$. This ensures that all of the wells are modeled in proper relation to each other.

2.4.2 Local and Regional Geology

The Lyondell Chemical Company, Channelview Plant site lies on the Texas Coastal Plain within the Houston Embayment of Southeast Texas. The structure of the area is characterized by a thick sequence of regionally southeast, gently dipping sediments and sedimentary rocks. The



GREENSBAY FRI 10 6 45 0
FIELD # 36728285

DEC 2000
OFFER #
163006

regional and local geology and hydrogeology are detailed in Section 4 of this 2000 HWDIR Exemption Petition Reissuance.

Correlation of disposal well logs, artificial penetration logs, and core samples indicate that there is no fracturing or faulting in the immediate vicinity the plant. However, correlation of disposal well logs and geophysical well logs from nearby oil and gas wells indicate that there is faulting southeast of the plant site, located just outside of the 2.5-mile radius Area of Review. These faults crosscut the Renee-Lynchburg Field structure, forming a series of three major down-to-the-basin normal faults.

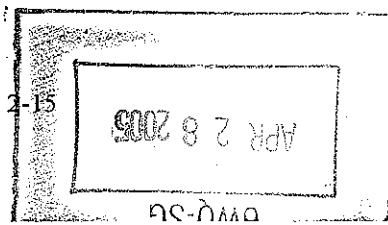
Injection currently occurs into Oligocene aged Frio sands (Frio E&F Sand) with an average depth of 6,750 feet (log depth) in both Plant Well 1 (WDW-148) and Plant Well 2 (WDW-162). Figure 2-2 shows a correlation of the lower Frio sands between the two facility wells currently used or proposed for the Lyondell Chemical Company, Channelview Plant.

Pleistocene to Miocene age deltaic sand and gravel deposits make up the principal ground-water aquifers in the Lyondell Chemical Company, Channelview Plant area. The base of the USDW (defined as <10,000 ppm total dissolved solids (TDS)) occurs at approximately 3,550 feet below surface elevation. Over 1,600 feet of shale and sand separate the injection zone from the lowermost USDW, with at least 350 feet of impermeable Anahuac Formation Confining Zone shale immediately overlying the Frio and Vicksburg Injection Zone.

2.4.3 Geologic Inputs to the Model

Prior to modeling, an understanding of the regional and local geology is essential. Based upon interpretation of conventional and sidewall cores, borehole geophysical logs, pressure measurements, laboratory tests, and in conjunction with published and unpublished literature, a comprehensive picture of the subsurface geology is developed for the plant site (see Section 4). Once the ranges of geologic parameters were established, conservative values are applied to mathematical models. Input parameters required by the flow and containment models are:

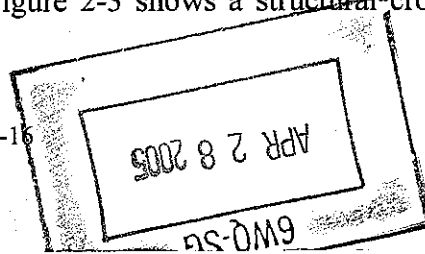
- Average sand and shale layer thickness
- Permeability of the sand and shale layers
- Porosity of the sand and shale layers



- Compressibility of the sand and shale layers
- Original formation fluid viscosity
- Original formation pressure
- Concentration Reduction Factor
- Free Water Diffusion Coefficient
- Effective Diffusion Coefficient
- Layer Dispersion Characteristics
- Boundary Conditions

General structural elements in the area surrounding the Channelview Plant are shown in Figure 4-22 (Structure Contour Map on the Vicksburg Marker, Section 4.0). Three northeast-southwest trending faults (along with their associated splinter faults) are located southeast of the plant. These faults transect the Renee-Lynchburg Field structure located south and southeast of the 2.5-mile radius Area of Review. The nearest fault is located slightly more than 12,500 feet southeast of the Channelview Plant (Top of the Frio A Sand, see Appendix 4-9). Additionally, a faulted piercement dome (Clinton Dome) is located approximately 8 miles west-southwest of the Lyondell Channelview Plant Figure 4-22 (Structure Contour Map on the Vicksburg Marker, Section 4.0). Geologic mapping of the dome (Section 4.0) shows that the structure is complexly faulted, which may form restrictions to fluid flow in that direction.

Therefore, a dual modeling strategy is employed to describe the geologic conditions at the Lyondell site. In the first modeling case (Case 1 – Sealed Fault A Case), the Renee-Lynchburg faults southeast of the facility are modeled as sealed, or non-transmissive, and the Clinton Dome structure is also conservatively bounded as a no flow barrier. This model case separates the Lyondell facility from the Houston Ship Channel area injection well sites. In the second case (Case 2 – Open Fault Case), all of the Renee-Lynchburg faults are modeled as non-sealed, or laterally transmissive (i.e., not a flow or pressure barrier). However, in this case the Clinton Dome structure is conservatively bounded and is still modeled as a no flow barrier. This model case allows the Houston Ship Channel area injection well sites to influence the Lyondell Chemical Company Channelview Plant. Figure 2-3 shows a structural cross section from the



Lyondell Channelview Plant to the Houston Ship Channel area injection wells. Figure 2-4 shows a structural cross section between the Houston Ship Channel area well facilities (extending from Shell (southwest) to Vopak (northeast) and includes the historical and current completions of these injection wells.

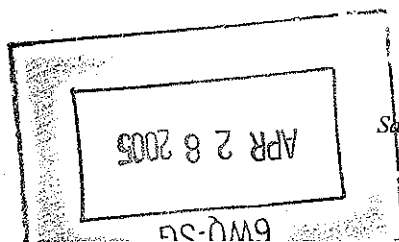
The Renee-Lynchburg Field faults are not vertically transmissive, due to the preponderance of sealing shale against shale present along the orientation of the fault plane in the Frio and Vicksburg Injection Zone and in the Anahuac Formation Confining Zone. The modeling assumption of lateral transmissivity (Case 2) is justified, however, since the lower Frio sands are not completely offset from the high-side to the low-side of the faults. This model case brings into potential pressure communication, all of the Houston Ship Channel area injection wells, which are also completed into the lower Frio sands. Modeling strategy is more fully developed in Section 2.5 in this 2000 HWDIR Exemption Petition Reissuance.

Table 2-1 shows the parameters used in the operational pressure model (*DuPont Multilayer Pressure Model*). This layer designation is used as the basic model setup. The current injection interval sand (Frio E&F Sand Injection Interval) is set up and modeled as a single layer (Layer 16) for pressure and plume geometry. The proposed Frio D (Layer 14) and the formerly used Frio A/B/C Sand (Layer 18) are also included as separate model units in the basic model setup. The injection interval sands are modeled as if they are encased in "tight" shales with an assigned low permeability of $1.0\text{E-}15$ darcies. This model assumption prevents pressure bleed-off through aquitards into the adjacent sands.

The *DuPont Vertical Permeation Model* uses the identical model layer and parameter assignments as the *DuPont Multilayer Pressure Model*, with the exception that the shale overlying the Frio D Sand (Shale Layer 13) is assigned an upper bound permeability of $1.7\text{E-}6$ darcies. In this model simulation run, the amount of vertical permeation is maximized, therefore, predicted vertical plume geometry is conservative.

The *DuPont Basic Plume Model* is a single layer model simulation based on assigned porosity-thickness (ϕ -h). Therefore, each of the three injection interval sands (Frio A/B/C Sand, Frio D Sand, and Frio E&F Sand) is modeled independently.

The following sections describe where and how the input parameters for the models are obtained.



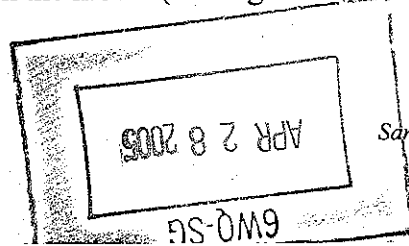
2.4.4 Layer Thickness

The *DuPont Basic Plume Model* and *DuPont Multilayer Pressure Model* perform two-dimensional computations for horizontal distribution of pressure and waste plume front boundaries. Therefore, they accept only one thickness value for each layer (in actuality, the *DuPont Basic Plume Model* is a true single-layer model). To determine appropriate average thickness values for each layer, geophysical logs and isopach maps over the entire region surrounding the plant are utilized.

The geologic model of the stratigraphic column employed in the present flow and containment calculations is a 20-layer conceptualization of the subsurface stratigraphy (see Table 2-1) from above the base of the lowermost usable source of drinking water to below the lower Frio injection sands. A type-log containing the Frio A/B/C Sand Injection Interval, the Frio E&F Sand Injection Interval, and the Frio D Sand Injection Interval is shown in Figure 2-5. These thicknesses (Table 2-1) are used in the *DuPont Multilayer Pressure Model* and the *DuPont Vertical Permeation Model*. Individual sand thicknesses used in the *DuPont Basic Plume Model* and the *DuPont 10,000 Year Waste Plume Model* are shown Table 2-2.

Thicknesses used for the *DuPont Basic Plume Model* and for the 200-year evaluation period for the High Specific Gravity Plume (*DuPont 10,000 Year Waste Plume Model*) are representative of the area surrounding the plant site and within the 2.5-mile radius Area of Review. Thicknesses used in the Low Specific Gravity Plume (*DuPont 10,000 Year Waste Plume Model*) are representative of the Victor Blanco and Alco-Mag Fields geographic area located directly north-northwest of the Area of Review (see Section 4.0 – Geology).

Analysis of well logs from the injection wells and other wells in the region, in conjunction with cross-section and isopach maps, indicates that the sand and shale layers are continuous and generally uniform in thickness over a geographic region much larger than the anticipated maximum waste plume extent (see Section 4.0). Where small-scale variations exist, such variations are not expected to materially influence model predictions, since their effects will tend to be averaged out over the larger distance scales. In terms of waste plume movement, the influence of small-scale variations in layer thickness is implicitly included within the framework of the dispersion parameters (i.e., "multiplying factor" in the Basic Plume Model and "dispersivities" in the 10,000-Year Waste Plume Model – see Section 2.4.10). Gross scale changes (i.e., reduction in effective sand thickness in the Frio B Sand and sand pinch-outs in the Frio D sand) are modeled as "no flow" barriers in the model (see Figures 2-15 and 2-19).



2.4.5 Transmissibility and Mobility

Transmissibility is defined as the permeability-thickness/viscosity product (kh/μ) and is a fundamental model input parameter. Mobility is defined as the capacity of a porous media to allow fluids to flow. Whole diameter cores and sidewall cores were taken during drilling of Plant Well 1 (WDW-148) give an initial assessment of permeabilities in the lower Frio sands and are included in Appendix 2-6. Additionally, the lower Frio Sands have been cored in Equistar's Plant Well 1 (WDW-36), Atofina's Plant Well 1 WDW-122) and Plant Well 2 (WDW-230), and Merisol's Plant Well 1 (WDW-147) and Plant Well 2 (WDW-319). These reports are also included in Appendix 2-6.

Although core samples provide a localized indication of relative permeabilities in the sands, transient well testing provides a more accurate determination of the overall formation transmissibility. Since 1990, Lyondell Chemical Company has conducted injectivity/falloff testing on the plant wells as part of its annual testing program. These tests have been re-evaluated for this 2000 HWDIR Exemption Petition and interpretation reports (and data diskette) are included in Appendix 2-6, Volume 4. From the falloff test data, transmissibility (kh/μ) of the injection interval can be directly calculated (Table 2-3, note that the listed transmissibilities are from the Superposition analysis). Additionally, from 1999 through 2002, an annual interference pulse test has been conducted in the Commingled Frio A/B/C Sand Injection Interval from Plant Well 2 (injector well) to Plant Well 1 (observation well) via a rate change at the conclusion of the falloff test in Plant Well 1 (WDW-148). These tests have also been re-evaluated for this 2000 HWDIR Exemption Petition and interpretation reports (and data diskette) are included in Appendix 2-6, Volume 4. From the interference test data, transmissibility (kh/μ) of the Frio A/B/C Sand Injection Interval can be directly calculated (Table 2-3). Note that the 1999 interference pulse and interference falloff test are of very short duration and may not be representative.

Transmissibility and permeability values, derived from injectivity/falloff tests are also available in the local area for the Frio E&F Sands (see Table 2-5). The Merisol Plant Well 1 (WDW-147), located approximately 6.2 miles southwest of the Lyondell Chemical Company, Channelview Plant, is completed solely in the Frio E&F Sand.

2.4.5.1 Layer Transmissibility in the DuPont Multilayer Pressure Model

Layer transmissibilities for the three injection intervals are determined from the annual

injection/falloff and interference tests. Assigned layer transmissibilities used in the pressure modeling are detailed below.

Frio A/B/C Sand Injection Interval

Results of the annual injectivity/falloff tests and the interference test results are shown in Table 2-3. Note that the tests conducted during 1991 through 1995 employed simultaneous shut-in of both injection wells. Therefore, these transmissibility values are considered to be "minimum" values, since the potential transient effects from the offset well are not considered in the analysis (no unique signal is available to show the cross-well influence during that time period). Simultaneous shut-in of the wells would result in a steeper Horner Slope during the radial flow period in the analysis of the raw data than if the offset well was not injecting or on continuous injection at a constant rate.

The 1991 through 1995, and 1997 through 2002 injectivity/falloff data in Plant Well 1 (WDW-148) and the 1992, 1993, and 1995 through 2002 injectivity/falloff data in Plant Well 2 (WDW-162) appear to represent the "best quality" data. Note that the two 1990 tests were run at a fairly low injection rate (approximately one-half the current test rates), for a fairly short injection period, and were run after the wells had been shut in for over two months, therefore, they may not be reflective of flow into the full thickness of the injection interval sands.

Transmissibility values, derived from injectivity/falloff tests, are also available in the local area for the Frio A/B/C Sand Injection Interval (see Table 2-5) from Merisol's Plant Well 2 (WDW-319). The Merisol well is located approximately 6.2 miles southwest of the Lyondell Chemical Company, Channelview Plant, and is completed solely in the Frio A/B/C Sand. Injectivity/falloff test data, which are analyzed in support of Merisol's underground injection control program, are presented in this 2000 HWDIR Exemption Petition Reissuance (see Appendix 2-6, Volumes 4 and 5). These data indicate a transmissibility range of 344,000 to 460,000 md-ft/cp for the Frio A/B/C Sand Injection Interval, with the exception of the 2001 falloff, which showed a reduced receptive interval taking flow. This low-value test in 2001 was remediated prior to the 2002 test by cleaning out and acidizing the well.

In order to be conservative in predicting pressure build-up during the operational period (historical and projected) of the wells, the transmissibility value of the Frio A/B/C Sand Injection Interval in this 2000 HWDIR Exemption Petition Reissuance is set to a value of 320,089.3 md-ft/cp (see Table 2-4). This value is generally below the lowest transmissibility calculated from

the annual injection/falloff tests conducted since 1992 and the three long-duration well-to-well interference pulse tests conducted in 2000, 2001, and 2002.

Frio E&F Sand Injection Interval

In April 2003, Plant Well 2 (WDW-162, was recompleted into the Frio E&F Sand injection interval. After a short-term injection period to build up pressure in the interval, a falloff test was run in the well to get a baseline transmissibility. Results of the test are included in Appendix 2-6, and indicate a transmissibility of 569,038.2 md-ft/cp. In April 2004, Plant Well 1 (WDW-148) was also recompleted into the Frio E&F Sand. Therefore, both an injection/falloff test and an interference pulse test were conducted in the Frio E&F Sand in 2004. Results of the falloff test in Plant Well 2 (WDW-162), note Plant Well 1 (WDW-148) maintained a steady rate fo 50 gpm through the test, indicate a transmissibility of 635,424.0 md-ft/cp, slightly higher than the initial 2003 test value. At the conclusion of the falloff in Plant Well 2 (WDW-162), the injection rate was rapidly increased from 50 gpm to 275 gpm. After 11.4 hours, Plant Well 2 (WDW-162) was shut-in and the falloff interference pressure also recorded. An analysis of the interference pulse buildup pressure is included in Appendix 2-6, and indicates an interwell transmissibility of 692,178.9 md-ft/cp (see Table 2-3). Testing was again performed in May 2005 using Plant Well 1 (WDW-148), with results indicating a transmissibility of 760,759.2 md-ft/cp. At the conclusion of the falloff in Plant Well 1 (WDW-148), Plant Well 2 (WDW-162) was shut in for an 8.3 hour duration and sthen injection was re-iniated at 275 gpm for a 14.4 hours. An analysis of the interference pulse buildup pressure is included in Appendix 2-6, and indicates an interwell transmissibility of 827,373.9 md-ft/cp (see Table 2-3).

Transmissibility values, derived from injectivity/falloff tests, are also available in the local area for the Frio E&F Sands (see Table 2-5) from Merisol's Plant Well 1 (WDW-147). The Merisol well is located approximately 6.2 miles southwest of the Lyondell Chemical Company, Channelview Plant, and is completed solely in the Frio E&F Sand. Injectivity/falloff test data, which are analyzed in support of Merisol's underground injection control program, are presented in this 2000 HWDIR Exemption Petition Reissuance (see Appendix 2-6, Volumes 4 and 5). These data indicate a transmissibility range of 319,000 to 872,000 md-ft/cp for the Frio E&F Sand, with all of the tests exceeding a transmissibility of 500,000 md-ft/cp, with the exception of the 1993 falloff.

Based on the initial and 2004 testing in Plant Well 2 (WDW-162), and considering the Merisol data, a conservative transmissibility value of 315,789 md-ft/cp is used for this sand in *DuPont*

Multilayer Pressure Model (Table 2-6).

Frio D Sand Injection Interval

Transmissibility of the Frio D Sand has not been directly measured in the area, since it is not a current injection interval at any of the near-by injection facilities. However, since its log characteristics are similar to sands of the Frio A/B/C Sand Injection Interval and the Frio E&F Sand Injection Interval, it is assigned a proportional transmissibility (87,719 md-ft/cp), based on its modeled thickness and formation fluid viscosity (Table 2-6).

2.4.5.2 Layer Mobility in the DuPont 10,000 Year Waste Plume Model

As shown in equations 1-a and 1-b in Appendix 2-5, the up-dip or down-dip velocity of the plume over the long term is controlled by the mobility (k/μ) input into the *DuPont 10,000 Year Waste Plume Model*. The best indicator of individual sand permeability comes from injectivity/falloff tests in the Frio E&F Sand in Lyondell's Plant Well 2 (WDW-162), interference testing to Plant Well 1 (WDW-148), and from Merisol's Plant Well 1 (WDW-147) [see Tables 2-3 and 2-5]. These wells are solely completed in the Frio E&F Sand, therefore; the "effective" receiving interval is known. The initial test in Plant Well 2 (WDW-162) showed a transmissibility of 569,038.2 md-ft/cp in the Frio E&F Sand. The 2004 injection/falloff test showed a transmissibility of 635,242 md-ft/cp and the calculated interwell transmissivity from the 2004 interference test is 692,178.9 md-ft/cp. Using a net thickness for the Frio E&F Sand of 155 feet and a viscosity value of 0.54 centipoise, these high-quality transient tests indicate an effective permeability of 1,982.5 millidarcies to 2,411.5 millidarcies in the Frio E&F Sand. Injectivity/falloff test data, which are analyzed in support of Merisol's underground injection control program, are also presented in this 2000 HWDIR Exemption Petition Reissuance (see Appendix 2-6, Volumes 4 and 5). These data indicate a transmissibility range of 576,800 to 872,000 md-ft/cp for the Frio E&F Sand in Plant Well 1 (WDW-147). Using a formation thickness of 215 feet at Merisol (the Frio E&F Sand is slightly thicker at Merisol) and a formation fluid viscosity of 0.54 centipoise, the effective permeability of the Frio E&F Sand ranges from 1,450 millidarcies to 2,190 millidarcies. These data are in good agreement with the transient tests in the Frio E&F Sand Injection Interval in Plant Well 2 (WDW-162) and the 2004 interference test from Plant Well 1 (WDW-148).

Merisol's Plant Well 2 (WDW-319) was drilled in 2000 and completed into the Frio A/B/C Sand

Injection Interval. Unlike the Frio E&F Sand completion in Merisol's Plant Well 1 (WDW-147), where the sand is blocky (as is the Frio E&F Sand at Lyondell) and the receptive thickness of the sand is constant and known, the Frio A/B/C Sand Injection Interval at Merisol is broken up horizontally by several shale breaks. These shale breaks may form partial horizontal barriers to flow in the interval, resulting in decreased receptive interval thicknesses, if certain of the perforation set are not receiving flow. The wellbore in Merisol's Plant Well 2 (WDW-319) has generally been open and accessible during testing. During the initial mechanical integrity testing of the well, and during the annual testing in 2001 and 2002, radioactive tracer velocity shots were taken in the longstring casing (9-5/8-inch casing) to determine the flow distribution throughout the completion. Since the flow profile within each perforation set is known, the receptive interval accepting flow during the transient testing is also known. Therefore, the effective permeability of the Frio A/B/C Sand can be determined from the transient test.

An analysis of the Merisol Plant Well 2 (WDW-319) data is presented in Appendix 2-6. To be conservative in the analysis of the transient tests, to determine a "maximum" effective permeability, the net effective sand thickness associated with each perforation set in Merisol's Plant Well 2 (WDW-319) was picked at a cutoff of 0.5 ohm-m on the 90-inch resistivity curve (open-hole well log). The conservative net sand associated with each perforation set was determined from the "0.5 ohm-m peak-to-peak" thickness in each sand lobe within which the perforations are contained. This methodology discounts a portion of the net sand within an individual lobe that is separated from the perforated interval by a horizontal resistive streak. The conservative net sand associated with each perforation set is tabulated in the analysis contained in Appendix 2-6. The three velocity profile data results (2000, 2001, and 2002) are also tabulated and presented. The 2000 flow profile shows that each of the perforation sets were open and taking flow, after initial completion and stimulation of the well. Note that in 2001, a diminished thickness of sand was taking flow. This is consistent with an observed increase in wellhead injection pressure for the well, even after several attempts to restore injection capacity to the well. In 2002, a through-tubing clean out and stimulation of the well was performed prior to conducting the annual testing. The cleanout and stimulation was effective in re-establishing the effective interval length taking flow in the well. A "*Net Calculated Receiving Thickness*" for each of the flow profiles was determined by conservatively assuming that any perforation set taking less than 5 percent of the flow had negligible contribution to the overall transmissibility of the falloff test. This "zeros-out" the uppermost Frio A/B Sand perforation set in the original well testing in 2000 and the uppermost Frio C Sand perforation set in the well testing in 2002. Additionally, the 2002 Net Calculated Receiving Thickness considers that only the uppermost

perforation set in the lower Frio C Sand lobe was open to flow since the final velocity shot was taken at 7,200 feet (log depth). This conservatively reduces the effective thickness by 28 feet (20 percent) for that survey.

The analysis in Appendix 2-6 includes a calculation of the maximum permeability for the three transient falloff tests conducted in 2000, 2001, and 2002. Note that there is a good correspondence between the transient falloff test derived transmissibility (permeability-thickness/viscosity product) and the calculated receiving interval thickness (i.e., the highest transmissibility test (original falloff in 2000) has the greatest receptive interval and the lowest transmissibility test (2001 falloff) has the smallest receptive interval). The conservatively calculated permeability for the 2000 and the 2002 falloffs are within 7 percent of each other, indicating an effective permeability of 1,734 millidarcies for the Frio A/B/C Sand Injection Interval.

These data bracket the range of lower Frio Sands to effective interval permeabilities of 1,450 to 2,400 millidarcies. In order to be conservative in predicting the maximum extent of plume drift during the post-operational period, the permeability of the Frio A/B/C Sand Injection Interval used in this 2000 HWDIR Exemption Petition Reissuance is set to a value of 2,500 millidarcies, which is equivalent to a long-term plume model mobility (k/μ) value of 4,629.63 md/cp using a viscosity of 0.54 cp. In order to be overly conservative in predicting the maximum extent of plume drift during the post-operational period, the permeability of both the Frio E&F Sand Injection Interval and the Frio D Sand Injection Interval is set to a higher value of 3,500 millidarcies in this 2000 HWDIR Exemption Petition Reissuance, which is equivalent to a long-term plume model mobility (k/μ) value of 6,481.48 md/cp using a viscosity of 0.54 cp.

2.4.5.3 Aquiclude (confining shale) Layer Permeability

Permeability values for the aquiclude layers (shale layers) in the 1990 HWDIR Exemption Petition are conservatively estimated from the literature (see Shale Porosity and Permeability in Appendix 2-6, Volume 5) and from measured vertical permeability data obtained during permitting of the DuPont Beaumont Works Plant Well 3 (WDW-188) located approximately 80 miles east of the Lyondell Chemical Company, Channelview Plant. The data is applicable to the Channelview site, as both wells penetrate identical geologic formations at similar depths and are part of the same structural subbasin. Data from this well is contained in Appendix 2-6, Volume 5 (see Groundwater Flow in Deep Saline Aquifers).

Shale permeability data from the DuPont Beaumont Works Plant Well 3 (WDW-188) can be confirmed in the local Harris County area from the Atofina Plant Well 2 (WDW-230). Whole core shale samples collected from 3,043.3 feet, 3,046.3 feet and 3,830.4 feet (Miocene), and 4,536.8 feet (Anahuac) in Plant Well 2 (WDW-230) were tested for vertical permeability (depths referenced to the open-hole log). The results are shown in Table 2-7. The results show permeabilities to brine of the shales in the Houston area to be less than 1×10^{-6} darcys, the limit of the testing method utilized. These values compare favorably with the upper end permeability values for the aquiclude or shale layers conservatively estimated from the literature values based on shale depth (Appendix 2-6, Volume 5 - see Shale Porosity and Permeability). For the *DuPont Multilayer Pressure Model*, permeability of the shales overlaying and underlying the injection interval sands are conservatively set to 1×10^{-15} darcies in order to prevent pressure "bleed-off" between permeable sand layers). For the *DuPont Multilayer Vertical Permeation Model*, permeability of the shale overlaying the Frio D Sand injection interval is conservatively set to 1.7×10^{-6} darcies in order to maximize permeation of waste and formation brine into the overlying shale layer. This value is significantly higher than the measured shale permeabilities in DuPont's Beaumont Well 3 (WDW-188) and is approximately twice the maximum permeability value measured in Atofina's Well 2 (WDW-230).

2.4.6 Porosity

Porosity is defined as the ratio of void space in a given volume of rock to the total bulk volume of rock expressed as a percentage. The more porous a rock the more fluid can be stored in a given rock volume. The porosity for each sand layer in the model are determined in this 2000 HWDIR Exemption Petition from sidewall core samples (see core reports in Appendix 2-6) taken in Plant Well 1 (WDW-148), with confirming values from Equistar Plant Well 1 (WDW-36), Merisol Plant Well 1 (WDW-147), and geophysical well log analysis. Average porosity values for the lower Frio Sands exceed 30 percent. The Litho-Density Porosity curve from the 1996 sidetrack in Plant Well 1 (WDW-148) was reviewed and confirms the assigned layer porosity data. To be conservative in the modeling of both pressure buildup and plume transport, a conservative porosity of 27 percent is assigned the Frio A/B/C Sand Injection Interval, the Frio E&F Sand Injection Interval, and to the Frio D Sand Injection Interval (Table 2-8).

2.4.6.1 Aquiclude (confining shale) Layer Porosity

Aquiclude layer porosities are determined from the correlations developed for Gulf Coast shales

(see Appendix 2-6, Volume 5 - Shale Porosity and Permeability) and confirmed with local data. Shale porosities are confirmed from data from Atofina's Plant Well 2 (WDW-230). Total bulk volume porosities obtained from whole core shale sample data in Plant Well 2 (WDW-230) are shown in Table 2-9. Note that the two higher porosity samples appear to be silts as opposed to true clays. This is based on the low abundance of total clay (17 percent) in the sample at 3,830.4 feet (referenced to the open-hole log depth).

The Array Induction Imager/Litho-density/Gamma Ray/Caliper log from the sidetrack hole of Plant Well 1 (WDW-148) was reviewed for supporting information on shale porosity. For a clean formation of known matrix density, the average formation bulk density (matrix material plus fluid) is expressed by (Schlumberger, 1987):

$$\rho_b = \phi \rho_f + (1 - \phi) \rho_{ma}$$

where:

ρ_b = is the bulk formation density

ϕ = is the porosity

ρ_f = is the fluid density

ρ_{ma} = is the formation matrix density

Solving for porosity:

$$\phi = \frac{(\rho_{ma} - \rho_b)}{(\rho_{ma} - \rho_f)}$$

The borehole of the sidetrack well is very ratty and uneven, which has a great effect on the pad tool readings of the Litho-density log (Appendix 2-6, Volume 3). However, good shale in relatively straight hole appears to occur at log depths between 6,494 to 6,500 feet and 7,070 to 7,090 feet. The bulk density read by the tool across these two areas is 2.25 to 2.3 gm/cm³. Assuming a formation fluid density of 1.05 gm/cm³ at reservoir conditions (typically a mud filtrate density of 1.0 gm/cm³ is used for porous, permeable intervals, however, since this is shale assume no infiltration) and a matrix density of 2.5 gm/cm³ for illite/smectite clays (Baroid, 1931), the calculated porosity for the 2.25 bulk density reading is:

$$\phi = \frac{(2.5 - 2.25)}{(2.5 - 1.05)}$$

$$\phi = 17.24\%$$

The bulk density value of 2.3 equates to a lower porosity of 13.8 percent.

In performing modeling calculations to predict an upper bound to the vertical distance of waste permeation (*DuPont Vertical Permeation Model*), it is conservative to employ a lower bound to the aquiclude layer porosity, as the extent of permeation is inversely proportional to the aquiclude layer porosity. The "effective" shale porosity, which discounts the bound water within the clay structure as well as water contained in dead end pores, represents an appropriate choice of a porosity value for such a calculation. A reasonable worst-case lower bound to the effective shale porosity as a function of depth for Gulf Coast shales is developed (see Appendix 2-6, Volume 5 - Shale Porosity and Permeability). The lower bound effective porosities (less than 10 percent) of the aquiclude layers used in this portion of the modeling are shown in Table 2-1 and are very conservative in comparison to local data.

In contrast to the vertical permeation calculation, the extent of vertical molecular diffusion of a contaminant species through the aquiclude layers overlying the injection sands is proportional to the aquiclude layer porosity, increasing roughly in direct proportion to the layer porosity. Therefore, in calculations to predict a conservative upper bound to vertical diffusion distance, a reasonable upper limit to porosity, such as the total shale porosity, should be used (see total porosity curves in Appendix 2-6, Volume 5 - Shale Porosity and Permeability). Frio aquicludes are conservatively expected to have a total porosity no greater than 21 percent based on the regional literature data, which is greater than the sidetrack Litho-density log calculated value of 17.24 percent. Molecular diffusion calculations employed in this 2000 HWDIR Exemption Petition Reissuance Request use this more conservative upper bound limit of 21 percent for shale porosity.

2.4.7 Original Formation Pressure

In the *DuPont Multilayer Pressure Model*, modeled pressure response with time is calculated as an incremental pressure change. Therefore, the model calculations are independent of actual depth. The calculated model pressure responses are then related back to the subsurface environment by assigning a reference pressure (original pressure) at a specific reference depth for each injection interval of interest. All site-specific pressure measurements (static shut-in

pressure and calculated flowing bottomhole pressure) are corrected to the injection interval reference depth (top of the injection interval sand), so that meaningful comparisons can be made between historical measurements and model response. For this 2000 HWDIR Exemption Petition Reissuance, a reference depth of 6,884 feet RKB is designated for the Frio A/B/C Sand Injection Interval, 6,625 feet RKB is designated for the Frio E&F Sand Injection Interval, and a reference depth of 6,510 feet RKB is designated for the Frio D Sand Injection Interval.

The best estimate of formation pressure in the Frio A/B/C Sand Injection Interval is determined from the collective static pressures measured in Plant Well 1 (WDW-148) and Plant Well 2 (WDW-162). These data are compiled in Appendix 2-6, Volume 4. Data since 1990 have been obtained during annual injection/falloff testing of the wells using both surface read-out and memory gauges run on wireline. Data pre-1990 was obtained on slickline using memory gauges and it is not always known if the offset injection well was operating or also shut-in. Therefore, a higher level of quality is assigned to the post-1990 pressure measurements. These static pressure data are compiled in Appendix 2-6, Volume 4, and presented in Figure 2-6. Note that the data in the Appendix 2-6 tabulation has been corrected to the injection interval reference depth for the Frio A/B/C Sand Injection Interval. In general, the static pressures have been taken at depths near the top of the interval; therefore, the measured pressures need only slight depth correction to the sand top reference depth.

The historical static pressures at the Frio A/B/C Sand reference depth of 6,884 feet RKB range from 2,849.3 psi to 3,052.12 psi. In the modeling, an original pressure of 2,971.2 psi at a reference depth of 6884 feet RKB is assigned in the Frio A/B/C Sand Injection Interval (average gradient of 0.432 psi/ft). This value is very close to the static pressure of 2,975.6 psi recorded in Plant Well 1 (WDW-148) during September 1990, after the wells had been shut-in for approximately three months, and should be very close to background conditions.

The original pressures in the Frio E&F Sand Injection Interval and the Frio D Sand Injection Interval were made calculated from the value used for the Frio A/B/C Sand Injection Interval using the specific gravity of 1.074 for the Frio Formation brines, accounting for the difference in the sand top depth. The adjustment of the measured pressure to the modeled mid-point depth was made using the following equation:

$$P_{adj} = (D_{new} - D_{P_{Frio A/B/C}}) * (0.4333 * SG_{fluid}) + P_{Frio A/B/C}$$

Where:

P_{adj} = Adjusted pressure at the new sand top depth (psi)

D_{new} = Depth at the new sand top (ft)

$D_{Frio\ A/B/C}$ = Top of Frio A/B/C Sand (ft)

SG_{fluid} = Specific Gravity of the formation fluid (dim)

$P_{Frio\ A/B/C}$ = Pressure for the Frio A/B/C Sand (psi)

For the overlying injection interval sands, the pressures were calculated at the following sand reference depths:

- 1) Frio E&F Sand - 6,625 feet; and
- 2) Frio D Sand - 6,510 feet.

For the Frio E&F Sand Injection Interval:

$$P_{E\&F} = (6,625\text{ ft} - 6,884\text{ feet}) * (0.4333 * 1.074) + (2,971.19\text{ psi})$$

$$P_{E\&F} = 2,850.66\text{ psi}$$

For the Frio D Sand Injection Interval:

$$P_D = (6,510\text{ ft} - 6,884\text{ feet}) * (0.4333 * 1.074) + (2,971.19\text{ psi})$$

$$P_D = 2,797.14\text{ psi}$$

The initial pressure of 2,877.9 psi measured at a reference depth of 6,625 feet in Plant Well 2 (WDW-162) following recompletion into the Frio E&F Sand (April 9, 2003) and the shut-in pressure of 2,872.0 psi following the initial falloff test on April 25, 2003 are in agreement with the model projections for the Frio E&F Sand at the Channelview Plant. Prior to any injection at Lyondell, the Sealed Fault A Case predicts a bottomhole pressure of 2,883.2 psi (Figures 2-78 and 2-79) at the reference depth of 6,625 feet and the Open Fault Case predicts a bottomhole pressure of 2,887.5 psi (Figures 2-90 and 2-91) due to offset injection at the nearby Class I sites. These modeled values exceed the measured values, indicating that the model is conservatively predicting pressure buildup in the Frio E&F Sand Injection Interval at the Channelview Plant.

2.4.8 Compressibility

Compressibility is defined as the change in volume per unit increase in pressure. In a zone that is 100% saturated with water, such as the disposal formation, the total compressibility is defined as the formation compressibility plus the compressibility of water corrected for water saturation:

$$c_t = c_f + c_w S_w$$

Formation compressibilities are determined from the early time match storativities determined from the 1999 through 2002 interference tests conducted from Plant Well 2 (injector) to Plant Well 1 (observation). Storativity is equal to the product of the formation porosity (ϕ), total compressibility (c_t), and formation thickness (h). An important component of storativity is the total compressibility (c_t). Petroleum engineering generally handles three-phases being present in a formation:

$$c_t = c_f + S_o c_o + S_w c_w + S_g c_g$$

where:

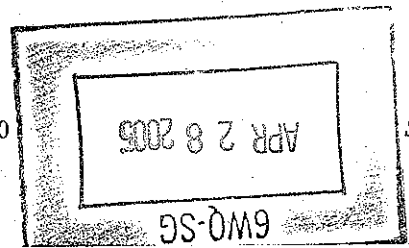
c_t	=	total compressibility (psi ⁻¹)
c_f	=	formation compressibility (psi ⁻¹)
S_o	=	oil saturation (fraction)
c_o	=	oil compressibility (psi ⁻¹)
S_w	=	water saturation (fraction)
c_w	=	water compressibility (psi ⁻¹)
S_g	=	gas saturation (fraction)
c_g	=	gas compressibility (psi ⁻¹)

For a water-filled reservoir, in which S_w equals 1, this simplifies to:

$$c_t = c_f + c_w$$

Storativities determined from the interference tests are shown below:

Test	Early Match Storativity (ft/psi)
------	-------------------------------------



Frio A/B/C

1999 Interference Pulse	5.05×10^{-4}
1999 Falloff Pulse	3.70×10^{-4}
2000 Interference Pulse	3.49×10^{-4}
2001 Interference Pulse	6.92×10^{-4}
2002 Interference Pulse	4.44×10^{-4}

Frio E/E 2004 INTERFERENCE TEST $\phi c_t = 9.638 \times 10^{-7}$ $\phi = .3$ $c_t = 3.2 \times 10^{-6}$

Using the minimum storativity of 3.49×10^{-4} ft/psi, a porosity of 31 percent for the Frio A/B/C Sand, and an effective receiving interval thickness of 160 feet, results in a calculated total compressibility (c_t) of 6.985×10^{-6} psi⁻¹.

In the DuPont Deepwell Models, the compressibility of water (c_f) is set to a fixed value of 3.035×10^{-6} psi⁻¹. Therefore, the formation compressibility (c_f) is equal to the calculated total compressibility (c_t) of 6.985×10^{-6} psi⁻¹ minus the water compressibility (c_f) of 3.035×10^{-6} psi⁻¹, or 3.950×10^{-6} psi⁻¹. In the *DuPont Multilayer Pressure Model*, formation compressibility is input as (α), which is defined in Freeze and Cherry (1979) (see Appendix 2-6, Volume 5) and is equal to the formation compressibility (c_f) times the formation porosity (ϕ). Using the formation compressibility (c_f) of 3.950×10^{-6} psi⁻¹ times the model input porosity of 27 percent, results in a *DuPont Multilayer Pressure Model* formation compressibility (α) of 1.07×10^{-6} psi⁻¹ for the Frio A/B/C Sand Injection Interval.

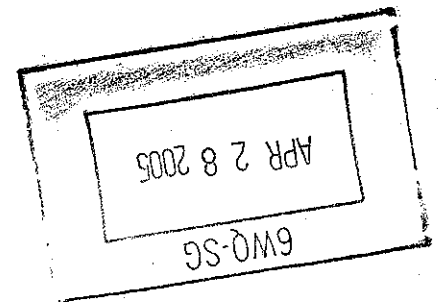
The employed sand compressibility value (α) is next compared to typical "oilfield" formation compressibilities (c_f).

In the oilfield, layer storativity (S) is typically defined as:

$$S_i = \rho g b_i c_i \phi_i$$

where:

- ρ = density of fresh water
- g = gravitational acceleration constant
- b_i = thickness of Layer i
- c_i = total compressibility of Layer i
- ϕ_i = porosity of Layer i.



For consolidated formations (i.e., "hard rock"), formation compressibility can be thought of as a modification of porosity that occurs when formation pore pressure changes:

$$c_f = \left(\frac{1}{\phi} \right) \left(\frac{\partial \phi}{\partial p} \right)$$

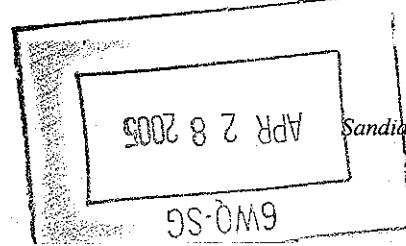
The change in porosity is a result of the elasticity of the solid structure of the rock. Correlations, such as presented in Hall (1953) and Van der Kamp (1959), are commonly used for these types of rock. Values of formation compressibility (c_f) are found to generally fall between $1 \times 10^{-6} \text{ psi}^{-1}$ and $10 \times 10^{-6} \text{ psi}^{-1}$ in consolidated formations (Hall, 1953; Van der Kamp, 1959; Earlougher, 1977, Newman, 1973).

However, for unconsolidated formations, the concept and magnitude of formation compressibility are quite different. In unconsolidated formations, the formation thickness distorts, or creeps, as the pore pressure changes. Evidence of this is the documented subsidence of the ground surface as hydrocarbons are produced over a long period of time in some fields (such as Spindletop, Wilmington, and Ekofisk). In unconsolidated formations, compressibility is defined as the change in pore volume, not just porosity:

$$c_f = \left(\frac{1}{V_p} \right) \left(\frac{\partial V_p}{\partial p} \right)$$

Laboratory tests can be performed on core samples, where the confining pressure surrounding the sample is increased and the volume of fluid squeezed out of the sample is measured (see, for example, Yale et al. (1993) in Appendix 2-6, Volume 5). Values for formation compressibility (c_f) generally lie in a range from $20 \times 10^{-6} \text{ psi}^{-1}$ to $100 \times 10^{-6} \text{ psi}^{-1}$ in unconsolidated formations (Wattenbarger, 1999, see Appendix 2-6, Volume 5).

Earlougher (1977) provides pore-volume compressibility data from Newman (1973) for 256 rock samples from 40 reservoirs (see Appendix 2-6, Volume 5). Yale et al. (1993) show over two orders of magnitude variation in formation compressibilities at a given pressure depending on the rock type (see Appendix 2-6, Volume 5). Newman (1973) found that in unconsolidated sands, pore-volume compressibility tends to increase with porosity, which is counter to the Hall correlation. The observed data range of formation compressibility for unconsolidated sands is from $3.5 \times 10^{-6} \text{ psi}^{-1}$ to $100.0 \times 10^{-6} \text{ psi}^{-1}$, with the general range being $20 \times 10^{-6} \text{ psi}^{-1}$ to in excess of $90.0 \times 10^{-6} \text{ psi}^{-1}$ (Newman, 1973) for sands with porosity greater than 30 percent.



Yale et al. (1993) provide a set of "type curves" for determining formation compressibility in unconsolidated sediments:

$$c_f = A(\sigma - B)^C + D$$

where:

- c_f = formation compressibility(psi^{-1})
- A = constant depending on rock type (1.054×10^{-4} for friable sands)
- B = constant depending on rock type (500 for friable sands)
- C = constant depending on rock type (-0.225 for friable sands)
- D = constant depending on rock type (-1.103×10^{-5} for friable sands)
- σ = effective stress

and:

$$\sigma = K_1\sigma_z - K_2p_i + K_3(p_i - p)$$

where:

- σ = effective stress
- σ_z = overburden stress
- K_1 = constant depending on rock type (0.95 for unconsolidated sands)
- K_2 = constant depending on rock type (0.95 for unconsolidated sands)
- K_3 = constant depending on rock type (0.75 for unconsolidated sands)
- p_i = original reservoir pressure (psi)
- p = present reservoir pressure (psi).

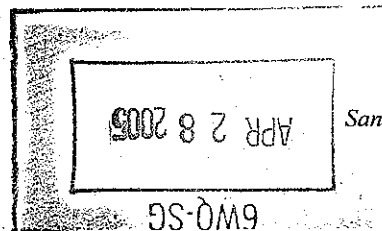
For the Frio A/B/C Sand, the calculation methodology (using the reference depth of 6,884 feet and a formation pressure of 2,971.19 psi) is outlined as follows. The initial step is to calculate sigma (σ). Using an overburden gradient of 1.0, the overburden stress at the sand is 6,884 psi. Calculating sigma at original formation conditions (i.e., no pressure change):

$$\sigma = 0.95 \times 6,884 \text{ psi} - 0.95 \times 2,971.19 \text{ psi} + 0.75 \times (2,971.19 \text{ psi} - 0)$$

$$\sigma = 5,945.6 \text{ psi}$$

Calculating the formation compressibility (c_f) using the friable variables:

$$c_f = 1.054\text{E-}04 \times (5,945.6 - 500)^{-0.225} - 1.103\text{E-}05$$



$$c_f = 4.6\text{E-}6 \text{ psi}^{-1}$$

Performing the appropriate unit conversions to solve for the relationship between oilfield formation compressibility (c_f) and hydrology formation compressibility (α):

$$c_f = \alpha / \phi$$

For the lower Frio Sands:

$$\alpha = 4.6\text{E-}6 \text{ psi}^{-1} * 0.27$$

$$\alpha = 1.2\text{E-}6 \text{ psi}^{-1}$$

Which is in good agreement with the compressibility value ($1.07 \times 10^{-6} \text{ psi}^{-1}$ for the Frio A/B/C Sand Injection Interval) determined from the interference testing.

In the *DuPont Multilayer Pressure Model* (see Appendix 2-2), compressibility is used within the calculation of layer storativity (S), with:

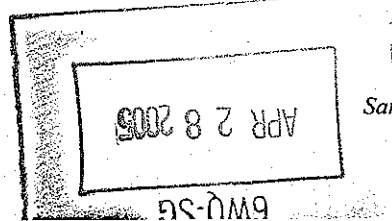
$$S_i = \rho g b_i (\alpha_i + \phi_i \beta_i)$$

where:

ρ	=	density of fresh water
g	=	gravitational acceleration constant
b_i	=	thickness of Layer i
α_i	=	compressibility of Layer i
ϕ_i	=	porosity of Layer i
β_i	=	compressibility of water.

This definition for storativity is the classic "hydrology" definition (Freeze and Cherry, 1979; Lohman, 1979). Both of these references are included in Appendix 2-6, Volume 5. Fluid (water) compressibility (β) is "hard-wired" into the FORTRAN code as $3.035 \times 10^{-6} \text{ psi}^{-1}$ after Table 2-5 in Freeze and Cherry (1979). A reproduction of Table 2-5 in Freeze and Cherry (1979) is included in Appendix 2-6, Volume 5 (as well as Table A1.3 that contains relevant unit conversions).

An example storativity calculation is provided for the Frio A/B/C Sand Injection Interval. Relevant input values from the .JOB file are a thickness of 150 feet (B(I)), a porosity of 27



percent (PHI(I)), and a compressibility (ALFIN(I)) of $1.07\text{e-}06 \text{ psi}^{-1}$. The first model conversion changes the input alpha value from units of psi^{-1} to units of feet^{-1} by multiplying the input ALFA value by 0.4333 psi/ft:

$$\text{ALFA(I)} = \text{ALFIN(I)} * 0.4333 \text{ psi/ft}$$

$$\text{ALFA(I)} = 1.07\text{e-}06 \text{ psi}^{-1} * 0.4333 \text{ psi/ft}$$

$$\text{ALFA(I)} = 4.636 * 10^{-07} \text{ feet}^{-1}$$

The compressibility of water is 'hard-wired' into the FORTRAN code as $1.315 * 10^{-06} \text{ feet}^{-1}$. Therefore, storativity in the model is calculated as follows:

$$S = B(I) * (\text{ALFA(I)} + 1.315\text{E-}6 * \text{PHI(I)})$$

$$S = 150 \text{ ft} * (4.636\text{e-}07 \text{ feet}^{-1} + 1.315\text{E-}6 \text{ feet}^{-1} * 0.27)$$

$$S = 1.228\text{E-}04$$

The calculated storativity for the Frio A/B/C Sand is also shown as $0.1228 * 10^{-03}$ in the .SUM output file under the "Derived Parameters" heading just prior to the time-step output summaries (see Appendices 2-7 and 2-8).

A storativity calculation is provided for the Frio E&F Sand Injection Interval in the following paragraphs. Relevant input values from the .JOB file are a thickness of 150 feet (B(I)), a porosity of 27 percent (PHI(I)), and a compressibility (ALFIN(I)) of $1.10\text{e-}06 \text{ psi}^{-1}$. The first model conversion changes the input alpha value from units of psi^{-1} to units of feet^{-1} by multiplying the input ALFA value by 0.4333 psi/ft:

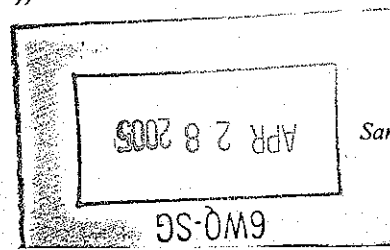
$$\text{ALFA(I)} = \text{ALFIN(I)} * 0.4333 \text{ psi/ft}$$

$$\text{ALFA(I)} = 1.10\text{e-}06 \text{ psi}^{-1} * 0.4333 \text{ psi/ft}$$

$$\text{ALFA(I)} = 4.766 * 10^{-07} \text{ feet}^{-1}$$

The compressibility of water is 'hard-wired' into the FORTRAN code as $1.315 * 10^{-06} \text{ feet}^{-1}$. Therefore, storativity in the model is calculated as follows:

$$S = B(I) * (\text{ALFA(I)} + 1.315\text{E-}6 * \text{PHI(I)})$$



$$S = 150 \text{ ft} * (4.766e-07 \text{ feet}^{-1} + 1.315E-6 \text{ feet}^{-1} * 0.27)$$

$$S = 1.248E-04$$

The calculated storativity for the Frio E&F Sand is also shown as 0.1248×10^{-03} in the .SUM output file under the "Derived Parameters" heading just prior to the time-step output summaries (see Appendices 2-7 and 2-8).

A storativity calculation is provided for the Frio D Sand Injection Interval in the following paragraphs. Relevant input values from the .JOB file are a thickness of 50 feet (B(I)), a porosity of 27 percent (PHI(I)), and a compressibility (ALFIN(I)) of $1.12e-06 \text{ psi}^{-1}$. The first model conversion changes the input alpha value from units of psi^{-1} to units of feet^{-1} by multiplying the input ALFA value by 0.4333 psi/ft:

$$ALFA(I) = ALFIN(I) * 0.4333 \text{ psi/ft}$$

$$ALFA(I) = 1.12e-06 \text{ psi}^{-1} \times 0.4333 \text{ psi/ft}$$

$$ALFA(I) = 4.853 \times 10^{-07} \text{ feet}^{-1}$$

The compressibility of water is 'hard-wired' into the FORTRAN code as $1.315 \times 10^{-06} \text{ feet}^{-1}$. Therefore, storativity in the model is calculated as follows:

$$S = B(I) * (ALFA(I) + 1.315E-6 * PHI(I))$$

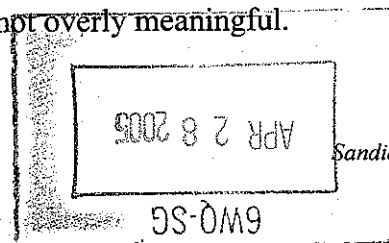
$$S = 50 \text{ ft} * (4.853e-07 \text{ feet}^{-1} + 1.315E-6 \text{ feet}^{-1} * 0.27)$$

$$S = 4.202E-05$$

The calculated storativity for the Frio D Sand is also shown as 0.4202×10^{-04} in the .SUM output file under the "Derived Parameters" heading just prior to the time-step output summaries (see Appendices 2-7 and 2-8).

2.4.8.1 Confining Shale Layer Compressibility

Confining shale compressibility (α) is conservatively assigned to be an order of magnitude higher in the base case pressure models. However, since the shale confining layers are made to be impermeable, choice of compressibility value is not overly meaningful.



In the *DuPont Vertical Permeation Model* runs, the shale layer overlying the Frio E&F Sand (Confining Layer 15) is conservatively assigned a compressibility (α) value of 7.0×10^{-5} psi⁻¹ (see Table 2-5 in Freeze and Cherry (1979)). This value is consistent with information included in Section 3.2.3 of Appendix 2-3 (see Appendix 2-3, Page 7).

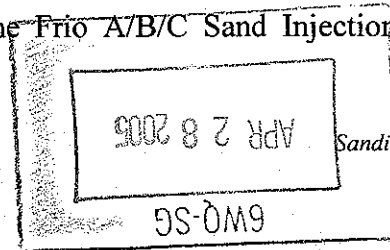
2.4.9 Temperature, Total Dissolved Solids, Viscosity, and Specific Gravity

2.4.9.1 Temperature

The subsurface formation temperature gradient in the East Houston area was initially estimated from a plot of the maximum temperatures recorded during open-hole logging operations in the nearby oil and gas wells. Site-specific formation temperature data is available from the September 1990 temperature log run in Plant Well 1 (WDW-148). Data from above the injection induced temperature anomaly in the lower Frio sands is plotted in Microsoft EXCEL[®] and fitted with a trend line (see Figure 2-7). These data show a gradient of 1.09 °F per 100 feet of depth, with a mean surface temperature of 81.1° F. This log is likely representative of background conditions since the Lyondell Chemical Company injection wells had been shut in since early July of that year. Maximum temperatures recorded during open-hole logging operations in the nearby oil and gas test wells are also included on Figure 2-7, and confirm the temperature profile data.

Additional temperature data is available from nearby Class I injection wells located at the Merisol Greens Bayou Plant, the Equistar Channelview Plant, and the Atofina Crosby Plant. These facilities are located on geologic trend with the Lyondell Chemical Company Channelview Plant (i.e. penetrate similar formations at similar depths). Data is available from the September 2000 temperature log run in Merisol's Plant Well 2 (WDW-319), the April 1994 temperature log run in the Atofina's Plant Well 2 (WDW-230), and the July 1988 temperature log run in the Equistar Plant Well 1 (WDW-36). The log from Merisol's Well 2 (WDW-319) and Atofina's Plant Well 2 (WDW-230) were taken on original installation of the wells and should be representative of background conditions. Equistar's Plant Well 1 (WDW-36) has only been infrequently used for injection since 1980; therefore, this log should also be representative of background conditions. Temperature logs are included in Appendix 2-6.

Data (for active wells, data from above the injection induced temperature anomaly) for these wells are also plotted in Microsoft EXCEL[®] (Figure 2-7). Each data set is fitted with a trend line. The range of reference temperatures for the Frio A/B/C Sand Injection Interval Sand



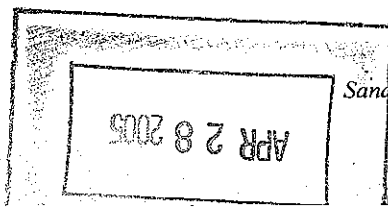
Injection Interval ranges from 145° F to 160° F at 6,884 feet (reference depth), the range of reference temperatures for the Frio E&F Sand Injection Interval ranges from 143° F to 156° F at 6,625 feet (reference depth), and the range of reference temperatures for the Frio D Sand Injection Interval is 142° F to 155° F at 6,510 feet (reference depth). To be conservative in the operational modeling, the coolest temperature is used in the determination of fluid viscosity (see Table 2-10).

2.4.9.2 Viscosity

Viscosity is the tendency of a fluid to resist flow. The DuPont Multilayer Pressure Model uses a single input value for the fluid viscosity within each modeled geologic layer. Therefore, the model assumes that the viscosity of the formation fluid and the injected waste fluid are identical (See Section 6.4 of Appendix 2-2). The effect of assuming that the waste viscosity is equal to the formation fluid viscosity will be relevant only within the borders of the waste plume. Outside the plume, the predicted pressure distribution will be virtually unaffected.

A formation fluid sample was taken from Plant Well 1 (WDW-148) during nitrogen backflow operations after initial perforating of the Frio A/B/C Sand Injection Interval (see Appendix 2-6, Volume 3). The sample is representative of "initial" undisturbed conditions in the lower Frio Sands. Total dissolved solids content of the recovered sample was measured to be 112,604 mg/l, with a NaCl content of 109,200 mg/l (see Appendix 2-6, Volume 3). Viscosity was determined from a nomograph of water viscosity at various temperatures and salinities (see Appendix 2-6, Volume 3). Note that the nomograph is scaled as a family of curves defined in terms of parts per million (ppm). Halliburton (1981) contains a conversion table for converting from parts per million to mg/l (see Appendix 2-6, Volume 3). For example, linear interpolation shows that 60,000 mg/l total dissolved solids content formation brine is equivalent to 57,500 ppm content formation brine. Linear interpolation of the 112,604 mg/l total dissolved solids in Plant Well 1 (WDW-148) converts to 104,828 parts per million brine. To account for all of the dissolved solids in the Frio Formation brine, Lyondell uses the total dissolved solids content of the fluid (112,604 mg/l), not just the NaCl content to determine the viscosity of the formation brine.

To be conservative in the prediction of pressure buildup, the lower-bound formation temperature is used (results in a more viscous fluid). The conversion to downhole formation temperature is illustrated on the nomograph and is equal to:



- 1) 0.56 centipoise in the Frio A/B/C Sand Injection Interval (temperature = 145° F at a reference depth of 6,884 feet);
- 2) 0.57 centipoise in the Frio E&F Sand Injection Interval (temperature = 143° F at a reference depth of 6,625 feet); and
- 3) 0.57 centipoise in the Frio D Sand Injection Interval (temperature = 142° F at a reference depth of 6,510 feet).

Viscosity for the injection intervals utilized in the operational models is summarized in Table 2-10. The viscosity of the fluids in the overlying layers is set to 0.60 centipoise in the model simulations. Since the overlying shales are made to be impermeable, the viscosity assigned to the shallower layers is inconsequential to the model results.

Viscosities used in the *DuPont Molecular Diffusion Model* are conservatively lowered to a conservative value of 0.44 centipoise. Use of this value in the diffusion modeling is overly conservative and will result in an overprediction of vertical transport.

Viscosities used in the *DuPont 10,000-Year Waste Plume Model* are conservatively lowered to a value of 0.54 centipoise in each of the injection intervals. Use of this value in the long-term plume transport modeling will result in an overprediction of horizontal transport. As shown in equation 1-a (the governing transport equation) in Appendix 2-5, the rate of plume transport DuPont 10,000 Year Waste Plume Model is directly proportional to the input mobility (k/μ) ratio (see also Section 2.4.9.3), not just the input viscosity variable. For Example, in the long-term modeling of the Frio E&F Sand, the DuPont 10,000 Year Waste Plume Model considered a mobility (k/μ) ratio of 6,481.48 md/cp. The initial falloff test in the recompleted Plant Well 2 (WDW-162) test indicates a mobility (k/μ) ratio of 3,671.2 md/cp, which is significantly less than the modeled value, using a conservative net thickness of 155 feet for the Frio E&F Sand. The mobility ratio modeled in the long-term transport demonstration exceeds that determined from annual falloff test, and therefore, modeled plume transport exceeds actual expected transport, all else being equal. Additionally, the long-term low specific gravity models do not consider the significant change in temperature that would occur from the approximate 1,500 feet change in structural elevation from the plant to Alco-Mag Field, located at the updip end of the long-term plume track. This is conservative as the formation fluid viscosities increase by just over 0.05 centipoise for each 10 degree decrease in temperature. The approximate formation temperature at Alco-Mag Field is 17 degrees cooler than at the Lyondell Plant.

2.4.9.3 Specific Gravity

Specific gravity of the fluids in the injection intervals primarily impacts the distance of lateral transport predicted by the *DuPont 10,000 Year Waste Plume Model*. As such, it is not an input into either the *DuPont Multilayer Pressure Model* or the *DuPont Basic Plume Model*. As shown in Appendix 2-5, the rate of long-term plume movement is governed by buoyancy forces, due to the difference between the formation fluid and modeled injectate. The governing equation can be simply written as:

$$U = \frac{k (\rho_w - \rho_f) g \beta}{2 \mu \phi}$$

See App 2-5
 See 13.B

where

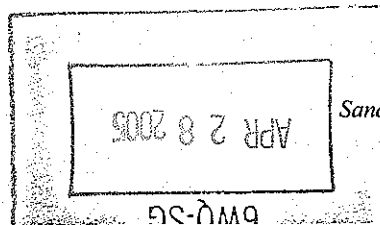
- β = dip angle below horizontal (radians)
- ρ_w = density of formation water,
- ρ_f = density of injectate water,
- g = gravitational acceleration constant,
- k = permeability
- μ = fluid viscosity
- ϕ = porosity

It is important to note that the rate of movement is not dependent on the absolute values of fluid densities (or therefore, the specific gravities), but only their difference. Therefore, as long as the difference is specified at a specific set of reference conditions (i.e., the same temperature), the calculation is valid. Lyondell conservatively uses the fluid specific gravities at the laboratory reference temperature of 60 °F in the long-term model calculations. As shown in Appendix 2-6 (see Density Nomograph, and Tables 3-29 and 3-90 from Perry and Chilton (1973)), the Microsoft EXCEL interpolation calculation example for the Frio Formation Brine and the low end requested running three-whole month average injectate specific gravity shows a greater density contrast at a temperature of 60° F than at downhole conditions of 145° F. Therefore, the DuPont 10,000-year Waste Plume Model will overpredict long-term plume transport.

See App 2-6

Formation Fluid

A formation fluid sample was taken from Plant Well 1 (WDW-148) during nitrogen backflow operations after initial perforating of the Frio A/B/C Sand Injection Interval (see



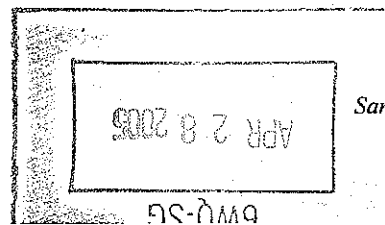
Appendix 2-6). The sample is representative of "initial" undisturbed conditions. Specific gravity of the recovered sample was measured to be 1.074. *60°F*

Injectate

Specific gravity of the injectate fluid is measured at a reference temperature of 60° F (see Section 1.8, Volume 1). A time series of measured twice-daily injectate specific gravities from January 1999 to March 22, 2005 is shown in Figure 2-9. A histogram of the twice-daily specific gravity data from January 1995 to March 22, 2005 is shown in Figure 2-10. The histogram shows that the majority of the daily data points fall within a narrow range, between 1.030 and 1.050. The volume weighted average average specific gravity value over the time period from January 1999 to March 22, 2005 is 1.042. Therefore, the average composite plume is slightly less dense than the formation fluid recovered from Plant Well 1 (WDW-148). Therefore, long-term plume movement will be up-dip to the northwest, away from the facility. The requested running three-whole month average specific gravity range at a temperature of 60° F is 1.028 to 1.100 in the Frio Injection Interval sands (approximates a 30,000 ppm NaCl brine to a 140,000 ppm NaCl brine). This results in a modeled High Specific Gravity Plume contrast of 0.026 (1.100 minus 1.074) and Low Specific Gravity Plume contrast of 0.046 (1.074 minus 1.028). Data shown on the time series graph indicates that the daily values have remained within the requested three whole-month volume weighted range over 95 percent of the time on an absolute basis. The calculated three whole-month volume weighted specific gravities (also shown on Figure 2-9) have historically fallen well within the requested range of specific gravities. ✓

(Fig 2-9, Vol 2)

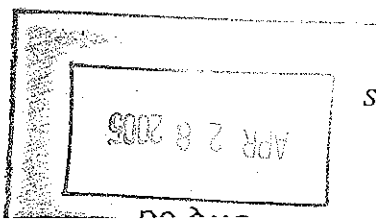
Conceptual modeling (Appendix 2-6, Volume 5) demonstrates that injectate plumes will travel as an average, both during operations due to mixing in the near-well area and during post-closure due to mixing with the drifting plume by dispersion (Fahy et al., 1992; Larkin et al., 1992; Larkin et al., 1993; Larkin et al., 1994). Specifically, Fahy et al, 1992, looked at the long-term dampening of single isolated pulses of anomalous densities (such as occur during large rain events) within the injectate plume. They show that the density anomaly is quickly dampened within a few hundred feet of the wellbore during continued injection and has no effect on long-term plume extent. Larkin et al. (1993), Larkin et al. (1994), and Larkin et al. (1994b) looked at the effects of "random" distribution of daily injectate densities versus the mean injectate density. Each of these studies found no significant difference in the extent of the model predicted long-term plume versus that predicted using the average value.



Additional conceptual modeling was conducted under a joint effort by DuPont, the Texas Chemical Council, and the EPA (Larkin, 1995). This study investigated the effects of short-term injectate stream density variations on long-term (10,000-year) plume movement. Specifically, Larkin (1995) looked at the effects of alternating densities on a quarterly basis (resulting in larger "slugs" of alternating densities). These studies were conducted to determine the viability of allowing deepwell operators the ability to employ a range of three-whole month injectate density averages in lieu of the more restrictive instantaneous injectate density limitation. The Texas Chemical Council worked closely with EPA staff in preparing the required modeling study simulation runs, which were compiled into a "*Modeling Effect of Input Parameter and Density Changes on Disposal Well Plumes*" report submitted by the Texas Chemical Council. EPA rightly concluded on July 19, 1995 (letter from Mr. Myron Knudson, Director Water Management Division to Mr. Mark Cheesman UIC Subcommittee Chair - Texas Chemical Council), that the modeling simulation runs successfully reinforced the results of previous studies. Therefore, a three-whole month volume weighted average injectate density is appropriate for facilities that do not inject "a significant amount of immiscible fluids." The Lyondell Chemical Company, Channelview Plant meets this criterion, as the injected stream is mostly water with minor quantities of dissolved salts and miscible organics (i.e., no free phase organics). Therefore, a "three-whole month volume weighted specific gravity range" is appropriate for the Channelview Plant.

2.4.10 Layer Dispersion Characteristics

The effects of non-uniformities within the sand bodies on the lateral transport and dispersion of waste during injection and long term post-injection are included differently in the *DuPont Basic Plume Model* and in the *DuPont 10,000-Year Waste Plume Model*. The *DuPont Basic Plume Model*, which describes waste plume growth during injection, employs the so-called "multiplying factor concept", developed by Miller, et. al. (1986) to place conservative upper bounds on the extent of advective/dispersive waste transport. This upper limit is most appropriate for the injection period, where the distance the waste travels from its source is relatively small, and where field scale Gaussian dispersion behavior is not approached (see Appendix 2-1 for an expanded discussion of lateral dispersion effects, and the applicability of the multiplying factor concept). The multiplying factor concept provides a more conservative upper bound to dispersion during the injection period than the conventional Gaussian "constant dispersivity" methodology. Furthermore, it is also designed to account for additional uncertainties and unquantifiable factors, such as injection interval anisotropy, on waste movement.



The *DuPont 10,000-Year Waste Plume Model* makes use of the conventional Gaussian "constant dispersivity" description. This methodology is appropriate in systems where the distance the waste moves from the source is large enough to achieve field scale Gaussian dispersion behavior.

2.4.10.1 Field Scale Dispersivities in DuPont 10,000-Year Waste Plume Model

In general, increasing travel distance equates to greater dispersion and, therefore, higher dispersivities. However, higher dispersivities allow the moving plume to spread out more (becoming more diffuse), which results in less transport. Xu and Eckstein (1995) (see Appendix 2-6, Volume 5) use a weighting scheme to analyze the relationship between field scale and dispersivity. By applying differing weighting schemes (from equal weighting to a 1:2:3 weighting for low, medium, and high reliability) based on reliability of data, they proposed three relationships between field scale and dispersivity:

$$\alpha_L = 1.20 \times (\log_{10} L)^{2.958}$$

1:1:1 Weighting Factor

$$\alpha_L = 0.94 \times (\log_{10} L)^{2.693}$$

1:1.5:2 Weighting Factor

$$\alpha_L = 0.83 \times (\log_{10} L)^{2.414}$$

1:2:3 Weighting Factor

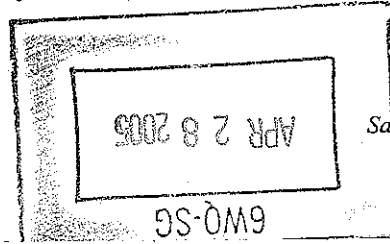
where:

α_L = longitudinal dispersivity (meters)

L = field scale (meters).

Therefore, an iterative process was used to model dispersivities in the long-term plume modeling. Initial estimates of the magnitude of transport distance for the leading edge of the injectate were made and an initial dispersivity assigned. Model results at the end of the evaluation period were then checked against the distance of anticipated transport, and adjustments were made in the model dispersivities, until modeled movement approximated anticipated movement.

The Low Specific Gravity long-term injectate plumes move approximately 70,000 feet to the north-northwest over their evaluation period (10,000 years). Based on this distance of movement, a lower-bound longitudinal dispersivity of 93 feet is considered in the base case Low



Specific Gravity Plume Models, and an upper bound longitudinal dispersivity of 300 feet is considered, as a sensitivity model run (Xu and Eckstein, 1995).

The High Specific Gravity long-term injectate plume moves approximately 10,000 feet to the southwest from the injection wells over its evaluation period (200 years). Based on this distance of movement, a lower-bound longitudinal dispersivity of 55 is considered in the base case High Specific Gravity Plume Model, and an upper bound longitudinal dispersivity of 157 feet is considered as a sensitivity model run (Xu and Eckstein, 1995).

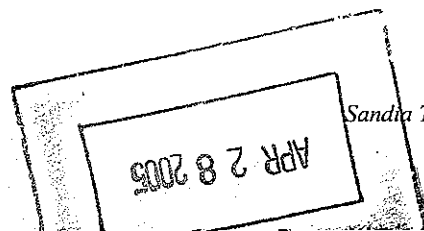
According to Walton (1985), the transverse dispersivity is commonly 5 to 10 times smaller than the longitudinal dispersivity. In the present calculations, a transverse dispersivity value of 10 time less than the longitudinal dispersivity feet is employed in the long-term modeling. Results from the *DuPont 10,000-Year Waste Plume Model* are fairly insensitive to the precise values specified for the field scale dispersion parameters.

2.4.10.2 Multiplying Factor for Advective Dispersion in DuPont Basic Plume Model

The "multiplying factor" M is used to describe advective dispersion in the *DuPont Basic Plume Model*. Calculation of waste plume growth during injection using the *DuPont Basic Plume Model* with the multiplying factor included (i.e., with $M > 1$) is designed to predict the maximum lateral extent possible for the waste plume. This is accomplished conceptually by tracking the movement of the fastest-moving portion of the waste.

The multiplying factor approach is implemented in practice by computationally assigning increased rates of injection to the various wells in the model, with values that have been enhanced by a factor of M . This produces computed velocities that have also increased by the same factor, M . The higher velocities correspond to the lateral speed of travel of the fastest-moving portion of the waste. Use of the *DuPont Basic Plume Model* combined with the multiplying factor provides a basis for tracking the location of this fastest-moving waste.

In the present calculations, the multiplying factor M has been specified on the basis of observed stratigraphic non-uniformities within the intervals employed for injection, determined from permeability variations of the core samples; it is also consistent with the field scale longitudinal dispersivity adopted in the *DuPont 10,000-Year Waste Plume Model*.



For perfectly stratified (layer cake) geological settings in which both the permeability and porosity vary solely with vertical depth through the injection interval, the multiplying factor can be calculated from the following formula (this equation is a simple extension of the earlier relationship developed in Miller, et. al. (1986) for geological systems in which only the

$$M = \frac{(k/\phi)_{\max}}{\frac{1}{h} \int_0^h (k/\phi) dz}$$

Core Data
located in App 2-6
Vol 3

permeability varies with depth):

where:

k = is the permeability at vertical location z

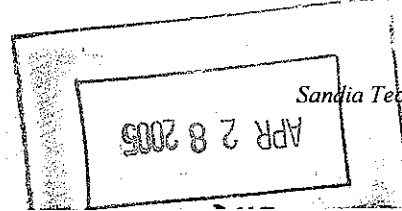
ϕ = is the porosity at z

h = is the thickness of the layer

As will be noted from this formula, the permeability k appears in both the numerator and denominator of the expression. This indicates that the absolute value of the permeability is not important in determining the multiplying factor. Only the variations of the permeability relative to the average value enter into the determination of M .

A variety of cores are available for the lower Frio sands from the Lyondell Chemical Company Channelview Plant, Merisol Greens Bayou Plant and the Equistar Channelview Plant; including sidewall cores and whole core data. Computation of the multiplying factor, based on geological considerations, was performed compositing the collective data from the Lyondell Chemical Company Channelview Plant, the Merisol Greens Bayou Plant, and the Equistar Channelview Plant. The calculation is made using the permeability/porosity pairs without any thickness weighting, and is presented in Table 2-11. The calculated Multiplying Factor is 3.8. ✓

These calculated values for M are, in the strictest sense, valid for a geological setting in which the only non-uniformities present are physical property variations with depth. However, in the actual geological setting at Channelview, the properties and thicknesses of the layers also vary



laterally, and the depositional system may exhibit anisotropy to some degree. These effects will tend to increase the predicted extent of the waste plume. On the other hand, the influence of transverse dispersion perpendicular to the bedding planes (i.e., vertically) will cause contaminants to move from higher to lower permeability depth increments within the injection interval, which will tend to reduce the extent of the waste plume. This transverse dispersion phenomenon is largely responsible for the transition that takes place from the purely advective dispersion existing in the near-well region, to the Gaussian dispersion, characteristic of the field scale.

It is significant that the multiplying factors are consistent with the conventional longitudinal dispersivity employed to describe lateral transport in the *DuPont Basic Plume Model*, as will next be demonstrated.

Consider a single isolated well injecting waste into a geological formation. The equations for combined advective and dispersive transport of contaminants in this system have been solved analytically by de Josselin de Jong (in Lau, et. al., 1959; see also Bear, 1972) for the case of conventional Gaussian dispersion. The approximate analytic solution obtained by de Josselin de Jong is in excellent agreement with the well-known numerical results of Hoopes and Harleman (1967). It is given by:

$$C = 0.5 \operatorname{erfc} \left(\frac{r - r_0}{\delta} \right)$$

$$\delta = \frac{2}{\sqrt{3}} \sqrt{\alpha_L r_0}$$

where:

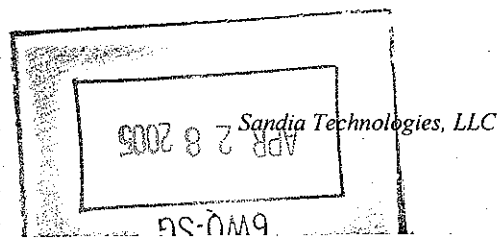
erfc = "complimentary error function"

C = relative contaminant concentration (normalized to the value in the waste stream) at radial distance (r) from the well

r_0 = "nominal" radius of the waste plume for a uniform formation without dispersion (feet)
 (i.e., calculated with $M = 1$)

δ = characteristic dispersion distance (feet)

α_L = longitudinal dispersivity (feet)



The relative concentration C required for the waste at Channelview to fall below health-based limits is $C = 1.0\text{E-}06$ (see Section 2.4.11.3). Substituting this value into the above formulas, and solving for the radial location r at which this concentration is attained in the injection interval sands, it is found that:

$$\frac{r}{r_0} = 1 + 3.36\sqrt{\alpha_L / r_0}$$

Dispersivity is a measure of the mechanical dispersion property of a porous material and is defined as a length to describe the ability of media to disperse solutes (Walton, 1985). Dispersivity is a function of both the vertical and lateral permeability variations and increases with formation heterogeneity. In general, increasing travel distance equates to greater dispersion, and therefore, higher dispersivities. Xu and Eckstein (1995) (see Appendix 2-6, Volume 5) use a weighting scheme to analyze the relationship between field scale and dispersivity. By applying differing weighting schemes (from equal weighting to a 1:2:3 weighting for low, medium, and high reliability) based on reliability of data, they proposed three relationships between field scale and dispersivity:

$$\alpha_L = 1.20 \times (\log_{10} L)^{2.958}$$

1:1:1 Weighting Factor

$$\alpha_L = 0.94 \times (\log_{10} L)^{2.693}$$

1:1.5:2 Weighting Factor

$$\alpha_L = 0.83 \times (\log_{10} L)^{2.414}$$

1:2:3 Weighting Factor

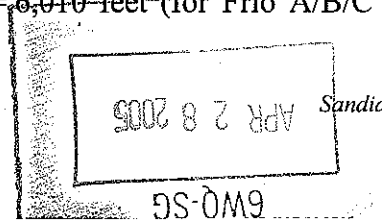
where:

α_L = longitudinal dispersivity (meters)

L = field scale (meters).

For the Lower Frio Sands, the largest nominal plume is encompassed by a radius of 6,010 feet at year-end 2020 (Frio A/B/C Sand Injection Interval). Calculated longitudinal dispersivities for the Lower Frio Sands are: 1) 1:1:1 Weighting Factor equals 129 feet; 2) 1:1.5:2 Weighting Factor equals 71 feet; and 3) 1:2:3 Weighting Factor equals 47 feet.

For a value of longitudinal dispersivity α_L equals 129 feet (largest dispersivity to be conservative) and a "nominal" plume radius of $r_0 = 6,010$ feet (for Frio A/B/C Sand Injection



Interval plume radii with $M=1$, conservatively assuming that all flow enters it), the above relationship predicts that:

$$\frac{r}{r_o} = 1.57$$

This indicates that the radial distance required for the waste concentration to fall below health-based limits will be 1.57 times the nominal radius of the plume. Since the multiplying factor M is a quantity based on volume of waste, the value of M necessary for the Basic Plume Model to predict this same radial distance for the outer boundary of the contaminant plume is given by:

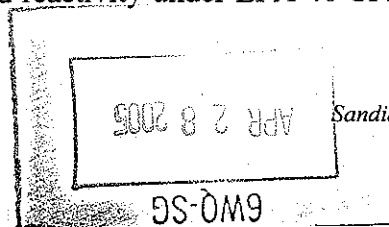
$$M = \left(\frac{r}{r_o} \right)^2 = 2.46$$

This result, derived for field scale Gaussian dispersion behavior, is significantly lower than the value $M = 3.8$ calculated from core samples and employed in the present calculations of waste plume growth during injection. Calculated Multiplying Factors for the Frio injection interval sands from Gaussian dispersion versus the modeled value are shown in Table 2-12.

Since Gaussian dispersion predictions are expected to provide upper bounds to the advective dispersion present in the region near the source (Walton, 1984; Molz, et. al., 1983), the calculation of waste plume growth using a multiplying factor of $M = 3.8$ is very conservative for all of the Frio injection interval sands. Based on this analysis, a value of 3.8 employed for the Multiplying Factor for each of the injection interval sands is very conservative. ✓

2.4.11 Waste Stream Characteristics

The Lyondell Chemical Company, Channelview Plant operates two Class I injection wells. The injected waste stream is a composite of several major process streams and consists of aqueous caustic solution with detectable quantities of organics. Prior to the promulgation of the Toxicity Characteristic (TC) rule (40 CFR 261, et. al., 55 Fed. Reg. 11798 (March 29, 1990)), the injected waste stream was regulated as a characteristic liquid hazardous waste due to corrosivity under EPA 40 CFR 261.22 (a)(1) (Waste Code D002) and reactivity under EPA 40 CFR 261.23 (a)(5)

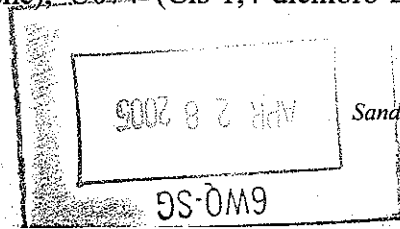


(Waste Code D003). These wastes, listed under EPA 40 CFR 268.12, were restricted from injection after May 8, 1992, without an approved Petition. The stream was petitioned for an exemption to the land disposal restrictions for EPA Hazardous Waste Numbers of D002 (corrosivity) and D003 (reactivity). EPA granted the exemption petition for D002 and D003 on June 29, 1990.

The promulgated Toxicity Characteristic rule (40 CFR 261, et. al., 55 Fed. Reg. 11798 (March 29, 1990)) created a new list of characteristic waste codes that are dependent on the concentration of organic constituents in the leachate from waste. After September 25, 1990, the injected waste stream at the Lyondell Chemical Company, Channelview Plant was also regulated as a characteristic liquid hazardous waste due the presence of benzene and methyl ethyl ketone and has additional EPA Hazardous Waste Numbers of D018 (benzene) and D035 (methyl ethyl ketone). Lyondell Chemical Company requested that D018 and D035 be added to the list of waste codes allowed for injection. At that time, Lyondell Chemical Company also requested that the ignitable characteristic (D001) and additional waste codes, which included acetone (U002), allyl alcohol (P005), benzene (U019), methanol (U154), methyl ethyl ketone (U159) and toluene (U220) (materials that may be present in the waste stream arising from *de minimis* losses) be added to the exemption. This HWDIR Exemption Petition Reissuance to add these streams was granted by EPA on March 24, 1992.

Lyondell Chemical Company requested that EPA Hazardous Waste Code F005 (Toluene) and U115 (Ethylene Oxide) be added to HWDIR Exemption Petition Reissuance Condition No. 5 during a second reissuance request. This second HWDIR Exemption Petition Reissuance to add these additional waste codes was granted by EPA on April 22, 1994.

Lyondell Chemical Company is requesting that additional EPA Hazardous Waste Codes be added as part of this 2000 HWDIR Exemption Petition Reissuance Request, for protective purposes. These codes are: D004 (Arsenic), D005 (Barium), D006 (Cadmium), D007 (Chromium), D008 (Lead), D009 (Mercury), D010 (Selenium), D011 (Silver), D022 (Chloroform), D026 (total Cresols), D028 (Ethylene Dichloride), F003 (spent Ethyl benzene and Methanol solvent), F005 (spent Acetone solvent and spent Ethyl benzene solvent), F039 (multi-source leachate), P003 (Acrolein), P013 (Barium), P047 (4,6-dinitro-o-cresol and salts), P065 (Mercury), P073 (Nickel), P074 (Nickel), P092 (Mercury), P099 (Silver), P103 (Selenium), P104 (Silver), P113 (Thallium), P114 (Selenium), P115 (Thallium), P119 and P120 (Vanadium), U001 (Acetaldehyde), U004 (Acetophenone), U031 (n-Butyl alcohol), U032 (Chromium), U051 (Xylene), U052 (Cresol, general), U055 (Cumene), U074 (Cis-1,4-dichloro-2-butene), U075

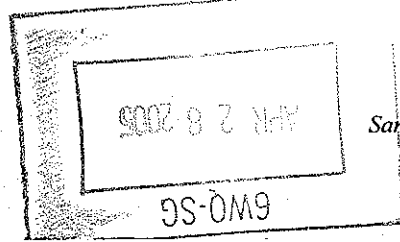


(Dichlorodifluoromethane), U077 (Ethylene dichloride), U136 (Arsenic), U140 (Isobutanol), U151 (Mercury), U165 (Naphthelene), U188 (Phenol), U204 and U205 (Selenium), U213 (Tetrahydrofuran), U214 through U217 (Thallium), U226 (1,1,1 Trichloroethane), and U239 (Xylene).

The rationale for including these additional EPA Hazardous Waste Codes are that they are present or may be present in materials on the plant site and could reasonably be present in the waste stream at some point in the future, arising from *de minimis* losses. EPA has not provided regulatory guidance on allowable *de minimis* concentrations; with a strict interpretation of the waste code carry thorough requirement, a small quantity of water that has contacted a listed waste, has the potential to render larger quantities of wastewater as hazardous. Additionally, potential spills or leaks of these materials create a resultant mixture that is also a hazardous waste according to the agency's interpretation of the "mixture rule". In this situation the spilled material, solid adsorbents, and any wash water used to remove the residual material from the impervious surface in the process area would also be classified as a hazardous waste by EPA. Thus, to ensure that all applicable waste codes are identified and approved for injection, Lyondell Chemical Company is requesting that these codes be added to the exemption.

The collective EPA Hazardous Waste Codes, including those requested in this reissuance, are tabulated below:

D Codes	D001, D002, D003, D004, D005, D006, D007, D008, D009, D010, D011, D018, D022, D026, D028, D035
F Codes	F003, F005, F039
P Codes	P003, P005, P013, P047, P065, P073, P074, P092, P099, P103, P104, P113, P114, P115, P119, P120
U Codes	U001, U002, U004, U019, U031, U032, U052, U051, U055, U074, U075, U077, U115, U136, U140, U151, U154, U159, U165, U188, U204, U205, U213, U214, U215, U216, U217, U220, U226, U239



2.4.11.1 Free Water Diffusion Coefficients

Diffusivities of organic and inorganic constituents of concern in free water solution that are evaluated in this 2000 HWDIR Exemption Petition are determined at reservoir temperatures using the high-quality predictive method for non-electrolytes in aqueous solutions employed by Hayduk and Laudie (1974) an ion in aqueous solutions employed by Lerman (1988). It is estimated that the uncertainties in these values are +10%, which translates into an uncertainty of +5% in the predicted diffusion distance. To maintain a high-level of conservativeness in the calculation, a lower bound fluid viscosity value of 0.44 centipoise is used in the transport modeling. The values employed in this 2000 HWDIR Exemption Petition Reissuance are shown in Table 2-13.

Free water diffusion coefficients for the constituents of concern, are calculated using the following methodology (see Appendix 2-6, Volume 5):

Example Problem

Benzene is a constituent of concern, determine the free water diffusivity at reservoir conditions using the method of Hayduk and Laudie (1974).

Example Solution

The method of Hayduk and Laudie (1974) is illustrated in the Handbook of Chemical Property Estimation Methods: Environmental Behavior of Organic Compounds (see Appendix 2-6, Volume 5). The applicable equation is :

$$D_{bw} = \frac{13.26 \times 10^{-5}}{\eta_w^{1.14} \times V_{B'}^{0.589}}$$

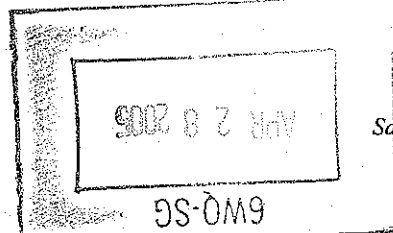
where:

D_{BW} = Free water diffusion coefficient

η_w = Viscosity of the formation fluid

$V_{B'}$ = LaBas molar volume of the constituent

The LaBas molar volume is calculated by summing the additive volume increment for each atom and adding a correction based on molecular structure; see Handbook of Chemical Property



Estimation Methods: Environmental Behavior of Organic Compounds Table 17-5 (see Appendix 2-6, Volume 5). For Example, for Benzene:

Atom	Increment (cm ³ /mol)	Number of Atoms			LaBas Molar Volume (cm ³ /mol)
Carbon	14.8	X	6	=	88.8
Hydrogen	3.7	X	6	=	22.2
6-Ring Molecule Correction					-15.0
V_B =					96.0

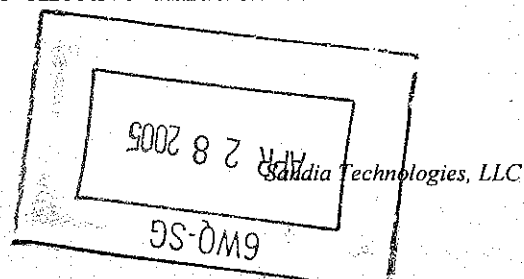
For the shales overlying the injection interval sands, a conservative formation fluid viscosity of 0.44 centipoise is chosen (approximately 12 percent reduction from the estimated value). Use of a lower viscosity will result in an overprediction of the free water diffusion coefficient. Substituting these values into the relevant equation:

$$D_{bw} = \frac{13.26 \times 10^{-5}}{0.44^{1.14} \times 96.0^{0.589}}$$

$$D_{\text{benzene}} = 2.30 \times 10^{-5} \text{ cm}^2/\text{sec}$$

2.4.11.2 Effective Diffusion Coefficients

According to the correlation given in Appendix 2-4, Volume 3, the geometric correction factor to account for the effects of complexities in the pore channel geometry on the effective diffusion coefficient is equal to or less than the square of the total aquiclude porosity. From Appendix 2-6, Volume 5 and Section 2.4.6, the total porosity of the shale overlying the shallowest injection reservoir is conservatively estimated to be no more than 21 percent. Therefore, based on the correlations developed in Appendix 2-4, Volume 3, the effective diffusion coefficient for the



molecules in the water saturated Frio aquiclude layers is no more than the free water diffusivities times the square of porosity (0.21^2). A example for benzene is shown below:

For shales overlying the Frio D Sand, a conservative estimate of the geometric correction factor G for contaminant diffusion through the water-saturated porous matrix is given by the relationship $G = \phi^2$. In the present case of $\phi = 0.21$, this results in an upper bound of 0.0441 for G . Since the diffusivity in free solution for benzene is $2.3 \times 10^{-5} \text{ cm}^2/\text{sec}$, the effective diffusion coefficient in the porous shale medium is:

$$D^* \leq 2.3 \times 10^{-5} \times (0.0441) = 1.01 \times 10^{-6} \text{ cm}^2/\text{sec}$$

Effective diffusion coefficients for all of the constituents of concern are shown in Table 2-13.

2.4.11.3 Concentration Reduction Factors

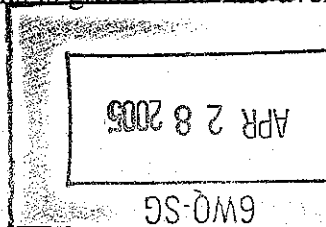
The concentration reduction factor for the constituents of concern is calculated by dividing the published health-based standard (or method detection limit) of the constituent by the maximum modeled concentration of the constituent. Maximum modeled concentrations greatly exceed those seen in the typical well feed (Appendix 1-1, Volume 1). Concentration reduction factors for the evaluated constituents are shown in Table 2-14. The limiting concentration reduction factor for this 2000 HWDIR Exemption Petition Reissuance is 1.0E-06. ✓

2.4.12 Formation Characteristics

2.4.12.1 Formation Dip Angle

Structuring of the geologic strata in the area is such that several prominent dip rate changes can be identified (see Figures 2-11 to 2-14) on the structure maps prepared and presented in Section 4.0. Specific "Top of Sand" maps are prepared for the Frio A Sand, the Frio C Sand, the Frio E&F Sand, and the Frio D Sand (see Appendix 4-9). In the immediate vicinity of the plant, the dip rate of the geologic strata is approximately 110 to 120 feet per mile, becoming slightly steeper in the down dip direction. In the updip direction, several dip rate changes are apparent (see Figures 2-11 to 2-14).

To be conservative in modeling the High Specific Gravity Plume, the dip rate for each of the injection intervals is set to -175 feet per mile. This is greater than the average dip rate measured



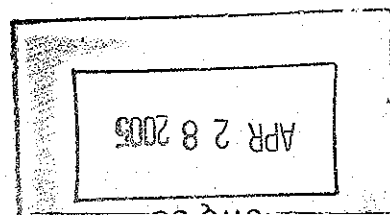
from the sand specific "Top of Sand" structure maps in the near-plant area, resulting in a conservative depiction of long-term plume movement.

The up dip rate of structural dip changes northwest of the facility are incorporated into the FORTRAN vectorizable code of the *DuPont 10,000 Year Waste Plume Model* by incorporating transition zones between the various dip rate changes. These changes are incorporated into the modeling via a sand specific .LCL file that is called by the *DuPont 10,000 Year Waste Plume Model*. Dip rates within the model are defined in the FORTRAN computer code (see Appendix 2-11, Volumes 18 through 20 - .LCL Files) as a series of nested "if" statements. The dip rate changes are detailed below for each of the modeled surfaces.

Frio AB Sand Surface

The updip dip rate changes displayed on the Top of the Frio A Sand (see Appendix 4-9) northwest of the facility are incorporated into the FORTRAN vectorizable code of the *DuPont 10,000 Year Waste Plume Model* by incorporating transition zones between the various regions of approximate "constant" dip. These changes are incorporated into the modeling via a sand specific .LCL file (FRIOAB.LCL) that is called by the *DuPont 10,000 Year Waste Plume Model*. Dip rates within the model are defined in the FORTRAN computer code (see Appendix 2-11, Volume 18 - .LCL Files) as a series of nested "if" statements, as follows:

```
if (X.gt.-22000.) then
  dipuse = -111.0
else if (X.gt.-26000.) then
  dipuse = -168. + 57.*(X+26000.)/4000.
else if (X.gt.-40000.) then
  dipuse = -168.
else if (X.gt.-44000.) then
  dipuse = -65. - 103.*(X+44000.)/4000.
else if (X.gt.-58000.) then
  dipuse = -65.
else if (X.gt.-62000.) then
  dipuse = -100. + 35.*(X+62000.)/4000.
else
  dipuse = -100.
end if
```



By model convention, X is a negative value in the updip direction, therefore, as the plume mass travels through each transition zone, the rate of structural dip progressively changes with increasing distance updip, until the new dip rate is achieved. Each new dip rate is then maintained until the next transition zone is encountered.

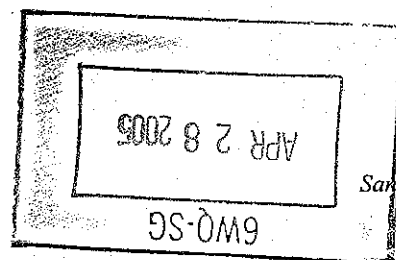
Frio C Sand Surface

The updip dip rate changes displayed on the Top of the Frio C Sand (see Appendix 4-9) northwest of the facility are incorporated into the FORTRAN vectorizable code of the *DuPont 10,000 Year Waste Plume Model* by incorporating transition zones between the various regions of approximate "constant" dip. These changes are incorporated into the modeling via a sand specific .LCL file (FRIOC.LCL) that is called by the *DuPont 10,000 Year Waste Plume Model*. Dip rates within the model are defined in the FORTRAN computer code (see Appendix 2-11, Volume 19 – .LCL Files) as a series of nested "if" statements, as follows:

```
if (X.gt.-22000.) then
  dipuse = -120.0
else if (X.gt.-26000.) then
  dipuse = -153. + 33.*(X+26000.)/4000.
else if (X.gt.-40000.) then
  dipuse = -153.
else if (X.gt.-44000.) then
  dipuse = -68. - 85.*(X+44000.)/4000.
else if (X.gt.-55000.) then
  dipuse = -68.
else if (X.gt.-59000.) then
  dipuse = -102. + 34.*(X+59000.)/4000.
else
  dipuse = -102.
end if
```

By model convention, X is a negative value in the updip direction, therefore, as the plume mass travels through each transition zone, the rate of structural dip progressively changes with increasing distance updip, until the new dip rate is achieved. Each new dip rate is then maintained until the next transition zone is encountered.

Frio E&F Sand Surface



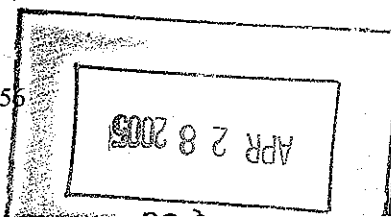
The updip dip rate changes displayed on the Top of the Frio E&F Sand (see Appendix 4-9) northwest of the facility are incorporated into the FORTRAN vectorizable code of the *DuPont 10,000 Year Waste Plume Model* by incorporating transition zones between the various regions of approximate "constant" dip. These changes are incorporated into the modeling via a sand specific .LCL file (FRIOEF.LCL) that is called by the *DuPont 10,000 Year Waste Plume Model*. Dip rates within the model are defined in the FORTRAN computer code (see Appendix 2-11, Volume 19 – .LCL Files) as a series of nested "if" statements, as follows:

```
if (X.gt.-22000.) then
  dipuse = -106.0
else if (X.gt.-26000.) then
  dipuse = -192. + 86.*(X+26000.)/4000.
else if (X.gt.-34000.) then
  dipuse = -192.
else if (X.gt.-38000.) then
  dipuse = -90. - 102.*(X+42000.)/4000. ✓
else if (X.gt.-46000.) then
  dipuse = -90.
else if (X.gt.-50000.) then
  dipuse = -35. - 55.*(X+50000.)/4000.
else if (X.gt.-62000.) then
  dipuse = -35.
else if (X.gt.-66000.) then
  dipuse = -113. + 78.*(X+66000.)/4000.
else
  dipuse = -113.
end if
```

By model convention, X is a negative value in the updip direction, therefore, as the plume mass travels through each transition zone, the rate of structural dip progressively changes with increasing distance updip, until the new dip rate is achieved. Each new dip rate is then maintained until the next transition zone is encountered.

Frio D Sand Surface

The updip dip rate changes displayed on the Top of the Frio D Sand (see Appendix 4-9) northwest of the facility are incorporated into the FORTRAN vectorizable code of the *DuPont 10,000 Year Waste Plume Model* by incorporating transition zones between the various regions of approximate "constant" dip. These changes are incorporated into the modeling via a sand



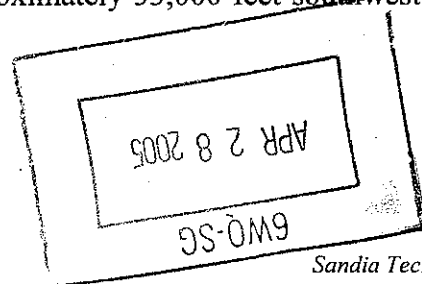
specific .LCL file (FRIOD.LCL) that is called by the *DuPont 10,000 Year Waste Plume Model*. Dip rates within the model are defined in the FORTRAN computer code (see Appendix 2-11, Volume 20 – .LCL Files) as a series of nested “if” statements, as follows:

```
if (X.gt.-20000.) then
  dipuse = -88.0
else if (X.gt.-24000.) then
  dipuse = -199. + 111.*(X+24000.)/4000.
else if (X.gt.-36000.) then
  dipuse = -199.
else if (X.gt.-40000.) then
  dipuse = -65. - 134.*(X+40000.)/4000.
else if (X.gt.-58000.) then
  dipuse = -65.
else if (X.gt.-62000.) then
  dipuse = -103. + 38.*(X+62000.)/4000.
else
  dipuse = -103.
end if
```

By model convention, X is a negative value in the updip direction, therefore, as the plume mass travels through each transition zone, the rate of structural dip progressively changes with increasing distance updip, until the new dip rate is achieved. Each new dip rate is then maintained until the next transition zone is encountered.

2.4.12.2 Formation Fluid Background Velocity

Many of the studies for flow rates in deep saline aquifers come from the search for nuclear waste isolation sites. These studies show sluggish circulation to nearly static conditions in the deep subsurface (see Appendix 2-6, Volume 5 - Groundwater Flow in Deep Saline Aquifers). Original formation pressure gradient data for the Frio Formation in the Channelview area substantiates the lack of a large hydraulic gradient within the basal Frio sands. Original formation pressure gradients from Lyondell Chemical Company, Plant Well 1 (WDW-148), from Equistar Plant Well 1 (WDW-36), located approximately 16,500 feet northwest, and from the Merisol Plant Well 1 (WDW-147), located approximately 33,000 feet southwest, are nearly identical (± 0.001 psi/feet).



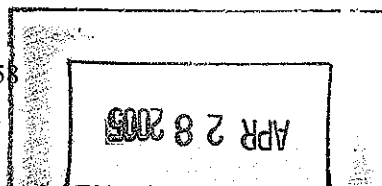
Lyondell Chemical Company presents literature data in Appendix 2-6, Volume 5 (see Groundwater Flow in Deep Saline Aquifers) showing that background velocities in the deep subsurface, in general, and in the Frio in particular, are generally less than 1.0 feet/year. To provide a greater margin of safety, Lyondell Chemical Company uses a conservative value of 1.62 feet/year as the maximum expected background velocity in the lower Frio. Lyondell Chemical Company believes that the background velocity of 1.62 feet/year is conservative (see Section 2.7.2.3). Since lateral facies changes, which result in sand pinch-outs, are known to occur in the direction of the recharge area, the background hydraulic gradient is greatly exaggerated in this 2000 HWDIR Exemption Petition Reissuance.

2.4.13 Boundary Conditions

Several geologic conditions exist in the area surrounding the Lyondell Chemical Company, Channelview Plant that may result in potential barriers to fluid flow. Although the injection interval sands are found to generally be continuous over the area investigated (see Section 4.0), several structural and stratigraphic complexities occur near the 2.5-mile radius Area of Review that may affect pressure build-up and plume geometry. The structural complexities include several down-to-the-basin normal faults that cross-cut the Renee-Lynchburg Field structure located south and southeast of the Channelview Plant, and faulting associated with the Clinton Dome piercement structure, located west of the plant. Stratigraphic complexities include areas of sand absence ("shale-out") of the Frio D Sand and the Frio B Sand. The potential boundary effects are detailed in the following subsections.

2.4.13.1 Renee-Lynchburg Field Fault Boundaries

A series of en-echelon down-to-the-basin normal faults are located south and southeast of the Lyondell Chemical Company, Channelview Plant (see Figure 4-22). These faults transect the Renee-Lynchburg Field structure, potentially offsetting the lower Frio injection interval sands. The closest fault (Fault A) is located approximately 12,500 feet south of Plant Well 1 (WDW-148) at the "Top of the Frio A Sand" (see Appendix 4-9). Fault A is delineated by a 150-foot fault cut in the Mitchell Energy, Houston Port Authority #1 well, a 100 -foot fault cut in the Amerada Hess Destec #2 well, a 175-foot fault cut in the Kelly Brock Kelly Brock Fee #1-A, and a 100-foot fault cut in the Gulf Coast Leaseholds Houston Ship Channel #1 well. Offsets on the Renee-Lynchburg faults range from 20 to 280 feet (see Section 4.0), with some of the larger displacement faults being capable of completely offsetting the injection interval sands. For the



Case 1 (Sealed Fault A Case) models, the closest mapped Renee-Lynchburg Field fault (Fault A) southeast of the Channelview Plant is conservatively considered to be laterally sealing (non-transmissive) and of infinite extent. In the Case 1 models, the implicit no-flow infinite fault boundary option available in the DuPont Models is employed. The implicit fault is defined by two coordinate points, located at $X_1=-16000$, $Y_1=-22000$, and $X_2=26000$, $Y_2=2000$.

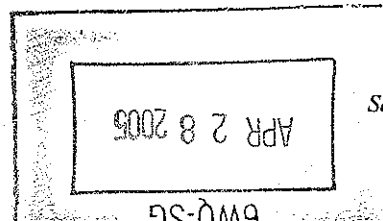
For the Case 2 models, the Renee-Lynchburg Field faults are considered to be laterally transmissive and, therefore, open to flow. The Case 2 models, therefore, allow for the possibility that the offset Class I injection wells south of the Houston Ship Channel (down-thrown side of Fault C) are in pressure communication with the injection interval sands utilized at the Channelview Plant. In the Case 2 models, the Renee-Lynchburg Field faults are not considered to be barriers to fluid flow or pressure communication.

2.4.13.2 Clinton Dome Boundaries

The second local structural feature that may influence pressure distribution and fluid flow is Clinton Dome, located approximately 8 miles west (crest of the feature) of the Lyondell Chemical Company, Channelview Plant. Geologic mapping of the dome (see Section 4.0) shows that the structure is complexly faulted, with radial faults emanating away from the crest. This structuring is typical of piercement-type structures. A central graben feature, that is open towards the Channelview Plant, is bounded by large displacement normal faults, located on the northeastern and southwestern sides of the graben block. Fault displacements of up to 340 feet occur in the field wells, and these large offset faults, in addition to the numerous smaller displacement faults, are likely to restrict or prevent fluid flow across the dome. Therefore, for each model case, Clinton Dome is conservatively modeled as a no flow barrier.

2.4.13.2.1 Clinton Dome Boundaries – Case 1 Models

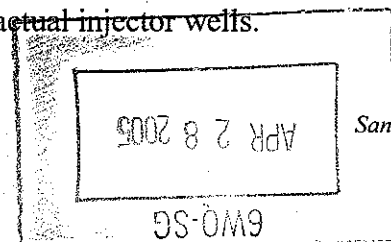
In the Case 1 models (Sealed Fault A Case), since the implicit no-flow infinite fault boundary option available in the DuPont Models is already employed for the trace of the Renee-Lynchburg Field Fault A, located south of the Channelview Plant, the boundary for Clinton Dome is modeled using a series of single-point injector wells that are active through the historical and projected time periods. Model input "image" injection wells are used in the Case 1 models to produce a boundary for Clinton Dome. The image wells are located and rate proportioned as determined following the "streamlines methodology" developed by Wattenbarger and Associates (see Appendix 2-6, Volume 3). The assumptions of the Streamline Model are the same as the



DuPont Models. That is, the reservoir is infinite, isotropic, homogeneous, constant thickness, and two-dimensional. Matthews, Brons, and Hazebroek (1954) used image well theory to develop drainage patterns for a number of difference drainage shapes. They used infinite numbers of image wells to calculate finite drainage areas. In applying their method to actual multi-well reservoirs, they showed that each well's drainage area is proportional to its flow rate, with no-flow boundaries being established between any two wells. For approximating no-flow boundaries in the DuPont model, a trial-and-error approach was taken to find the rates and locations of image wells that would approximate estimated actual boundaries. When the image well was correctly placed at the correct rate, none of the streamlines from the actual injection well would cross the desired no-flow boundary. Likewise, none of the streamlines from the image wells cross the no-flow boundary.

The injector wells are located and the injection rates are defined, such that a "constant" no flow boundary coincident with a modeled Clinton Boundary exists during modeled injection (see Appendix 2-6). In this way, the volumetric two-dimensional reservoir area (injection area) available for flow northwest of the model implicit Fault A is constant through time. The injection area of a well can be defined as the area invaded by the injected fluid, given enough time (infinite time). This area can be found by tracing the ray-paths of all of the injection fluid particles. For example, if 360 particles are originated surrounding an injection well, each located 1 degree apart to represent 360 degrees around the well, then the resultant family of connected particle tracks (or streamlines) at infinite time, would cover the injection area of the well. This particle tracking for the streamlines is identical to the procedure employed in the *DuPont Basic Plume Model*. Therefore, the *DuPont Basic Plume Model* can be used to simulate the "injection area" of each well.

The outermost streamline paths coincide with "boundaries" of the injection area. In actual injection wells, these boundaries may be combinations of sealing faults, pinch-outs, or interference boundaries with other actual injection wells. For approximating the Clinton Dome no-flow boundary for the DuPont models, a trial-and-error approach was taken in the *DuPont Basic Plume Model* to find the rates and locations of Clinton injector wells that would approximate the modeled Clinton Dome boundary. For a particular well trial, various streamlines were constructed by choosing a location in the injection area of a particular well – then the streamline from that location was calculated using the *DuPont Basic Plume Model*. When the Clinton injector well is correctly placed, and the injection rate is properly set, none of the streamlines from the actual Class I injection wells cross the desired no-flow boundary simulating Clinton Dome. Likewise, none of the streamlines from the Clinton injector well would cross the same no-flow boundary with the actual injector wells.

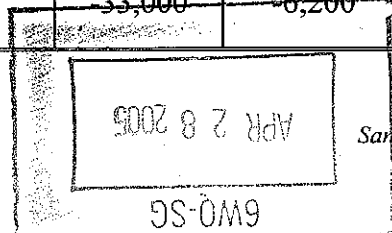


The location of the streamlines is not affected by injection rate changes, as long as the Clinton injector well changes its rate in the same proportion as the actual injection wells. So, for example, the injection well rates can change monthly without affecting the location of streamlines (and modeled no-flow boundary) if the relative rates with the Clinton injector well are preserved. However, if the rate changes are of a non-proportional manner, then the available injection area (and modeled no-flow boundary) will change. This is also true if the locations of the injection wells change with time. A new streamline pattern will be established after a short transient readjustment time has passed. If the change in injection areas is fairly small (i.e., small change in injection well location or rate proportion), then this type of rate change may still be a reasonable approximation, without a need to readjust the model. Such a change might occur when adding a well in close proximity to an existing well, shutting in a well, or changing the injection ratio between actual wells. For the current development, each time a new Class I injection well was completed into the sand being modeled, the Clinton injector well location and rate was evaluated, and modified, such that desired no-flow boundary location simulating Clinton Dome was maintained.

The modeled Clinton no-flow boundary in the Case 1 models follows the approximate projection of the -6,200-foot contour, as identified on the "Top of the Frio E&F Sand Structure Map" (see Appendix 4-9). This contour is projected around the dome, resulting in a curved boundary surface in the Case I models. The modeled boundary conditions in the Case 1 models are shown in Figure 2-15. For the Frio A/B/C Sand Injection Interval, the historical modeled injection area is affected by offset injection at Equistar (WDW-36), Merisol (WDW-319), and Lyondell (WDW-148 and WDW-162), and to a lesser extent by Atofina. The projected case model (2002 through 2020) is also affected by all of these wells. Note that the Equistar well has not been used on a sustained basis since 1980, therefore, modeling a future rate for this well is conservative.

Four Clinton Dome injection wells were defined for the historical time period and one well is defined for the projected time period in the Frio A/B/C Sand Injection Interval:

Model Period	Time Period	Clinton Injector Well	Location X	Location Y	Flow Proportion
Equistar Only	03/69 - 06/78	D1	-34,000	-5,000	26%
Lyondell & Equistar	07/78 - 9/80	D2	-33,000	-6,200	25.5%



Lyondell Only	10/80 - 12/00	D3	-32,750	-7,200	25.5%
Merisol & Lyondell	01/01 - 12/01	D4	-32,500	-10,000	31.1%
Projected*	01/02 - 12/20	D5	-32,500	-10,500	30.1%

* Projected = Merisol, Lyondell, Equistar, Cobra, and Atofina at maximum rates

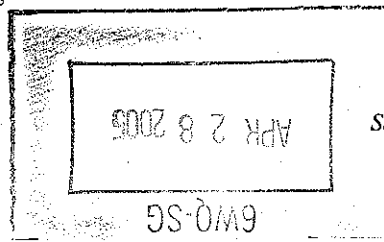
The *DuPont Basic Plume Model* was used to define the "injection area" of each well (actual well and Clinton Dome Boundary Well). The results for the five time periods in the Frio A/B/C Sand Injection Interval Case 1 Model are shown in Figure 2-16.

For the Case 1 Frio E&F Sand Injection Interval models, the historical modeled injection area is affected by offset injection at Equistar (WDW-36) and Merisol (WDW-147), and to a lesser extent by Atofina. The modeled injection area in the projected Case 1 Frio E&F Sand Injection Interval models are also affected by injection into the Frio E&F Sand at Lyondell. To be overly conservative in the modeling of the Frio E&F Sand, Equistar's Plant Well 1 (WDW-36) is included in the projected modeling. This well has not been used on a sustained basis since 1980 and would likely only be used in the event that both Plant Well 1 (WDW-148) and Plant Well 2 (WDW-162) were inoperative (the Equistar stream is currently injected into Lyondell's wells, see Section 1). A total of four Clinton Dome injection wells were defined for the historical and projected time periods in the Frio E&F Sand, as follows:

Model Period	Time Period	Clinton Injector Well	Location X	Location Y	Flow Proportion
Equistar Only	05/77 - 07/79	D1	-34,000	-5,000	26%
Merisol & Equistar	08/79 - 09/80	D2	-33,500	-8,000	24.8%
Merisol Only	10/80 - 12/01	D3	-31,500	-12,500	37.5%
Projected*	01/02 - 12/20	D4	-32,500	-10,500	30.1%

* Projected = Merisol, Lyondell, Atofina, and Equistar at maximum rates

The *DuPont Basic Plume Model* was used to define the "injection area" of each well (actual well and Clinton Dome Boundary Well). The results for the four time periods in the Frio E&F Sand Injection Interval Case 1 Model are shown in Figure 2-17.



2.4.13.2.2 Clinton Dome Boundaries – Case 2 Models

In the Case 2 models, the implicit no-flow infinite fault boundary option, available in the DuPont Models is employed for the Clinton boundary. The implicit fault is defined by two points in the Case 2 models, located at $X_1=-34000$. $Y_1=-20000$., $X_2=-26000$. $Y_2=-6000$. This allows for an easier placement of the Clinton Dome Image Wells, as the model correctly places the image well locations and injection rates. The modeled boundary conditions in the Case 2 models are shown in Figure 2-18.

2.4.13.3 Potential Sand Shale-out Boundaries

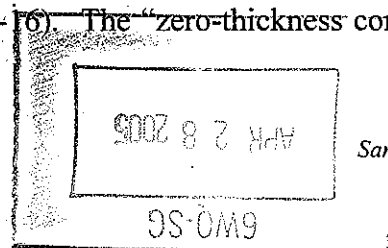
Geologic mapping of the lower Frio sands shows that they are generally continuous through out the study area. However, the Frio B Sand thins to the west of the Channelview Plant and is absent across portions of the Clint Dome structure. Additionally, the Frio D Sand shows several areas of sand absence in the area. Therefore, for model cases, these potential flow restrictions due to stratigraphy are considered in the modeling.

2.4.13.3.1 Frio B Sand

In the models, since the approximate location of the shale out in the Frio B Sand is coincident with the complex structuring due to the radial faulting across Clinton Dome, this potential stratigraphic boundary is already considered in the models.

In the Case 2 models, the implicit no-flow infinite fault boundary option available in the DuPont Models is employed for the Clinton boundary/Frio B Sand pinchout. The implicit fault is defined by two points in the Case 2 models, located at $X_1=-34000$. $Y_1=-20000$., $X_2=-26000$. $Y_2=-6000$. This allows for an easier placement of the Clinton Dome/Frio B Sand Pinchout Image Wells, as the model correctly places the image well locations and injection rates. The modeled boundary conditions in the Case 2 models are shown in Figure 2-18. The projected Case 2 model (2002 through 2020) in the Frio A/B/C Sand is also affected by all of the offset wells. Note that the Equistar Plant Well 1 (WDW-36) has not been used on a sustained basis since 1980 and would only be used in the unlikely event that both Plant Well 1 (WDW-148) and Plant Well 2 (WDW-162) were inoperative (the Equistar stream is currently injected into Lyondell's wells, see Section 1), therefore, including this well in the model is very conservative.

The modeled Clinton no-flow boundary in the Case 1 models follows the approximate location of the pinchout in the Frio B Sand (see Figure 4-16). The "zero-thickness contour is projected



around the dome, resulting in a curved boundary surface in the Case I models. The modeled boundary conditions in the Case I models are shown in Figures 2-15 through 2-17. For the Frio A/B/C Sand Injection Interval, the historical modeled injection area is affected by offset injection at Equistar (WDW-36), Merisol (WDW-319), and Lyondell (WDW-148 and WDW-162), and to a lesser extent by Atofina. The projected case model (2002 through 2020) is also affected by all of these wells. Note that the Equistar Plant Well 1 (WDW-36) has not been used on a sustained basis since 1980 and would only be used in the unlikely event that both Plant Well 1 (WDW-148) and Plant Well 2 (WDW-162) were inoperative (the Equistar stream is currently injected into Lyondell's wells, see Section 1), therefore, including this well in the model is very conservative.

Four Clinton Dome/Frio B Sand Pinchout injection wells were defined for the historical time period and one well is defined for the projected time period in the Frio A/B/C Sand Injection Interval:

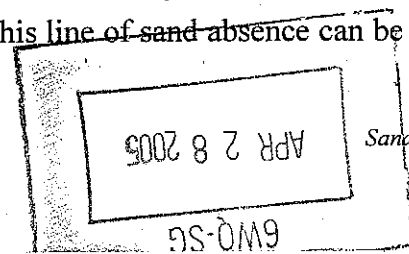
Model Period	Time Period	Clinton Injector Well	Location X	Location Y	Flow Proportion
Equistar Only	03/69 - 06/78	D1	-34,000	-5,000	26%
Lyondell & Equistar	07/78 - 9/80	D2	-33,000	-6,200	25.5%
Lyondell Only	10/80 - 12/00	D3	-32,750	-7,200	25.5%
Merisol & Lyondell	01/01 - 12/01	D4	-32,500	-10,000	31.1%
Projected*	01/02 - 12/20	D5	-32,500	-10,500	30.1%

* Projected = Merisol, Lyondell, Cobra, Atofina and Equistar at maximum rates

The *DuPont Basic Plume Model* was used to define the "injection area" of each well (actual well and Clinton Dome Boundary/Frio B Sand Pinchout Well). The results for the five time periods in the Frio A/B/C Sand Injection Interval Case I Model are shown in Figure 2-16.

2.4.13.3.2 Frio D Sand

The Frio D Sand shows several areas of sand absence to the southwest of the Channelview Plant (see Figure 4-18). These areas of sand absences form a rough northwest to southeast line near the 2.5-mile radius Area of Review boundary. This line of sand absence can be projected across



the southwestern portion of the 2.5-mile radius Area of Review to intersect the modeled Fault A linear barrier, thereby, resulting in two potential no flow barriers in the Case 1 models for the Frio D Sand. In general, dealing with two intersecting boundaries can be computationally difficult. The best case is when intersecting barriers can be approximated by a wedge and the ratio of 360° /"wedge angle" is an even integer. In this case, the image wells come back around full circle to the injection well. The number of image wells required is obtained from the following equation (DuPont, 1999):

$$NIW = ((360^\circ / (\text{wedge angle})) - 1) * NWELL$$

where:

NIW = Number of Image Wells

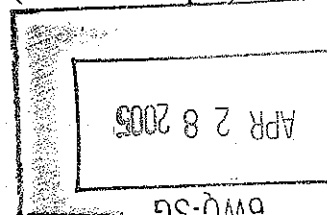
NWELL = Number of Injection Wells

For computational ease in the Case 1 modeling of the Frio D Sand Injection Interval, an angle of intersection of 120° is used for the two-modeled linear no-flow barriers and a single injection well is used. This results in two image well locations needed to properly image the Lyondell injection well $((360^\circ \text{ divided by } 120^\circ) - 1)$. *Access w/ Pan System*

A schematic drawing of the Case 1 model boundaries in the Frio D Sand is shown in Figure 2-19.

2.4.14 Waste Disposal History

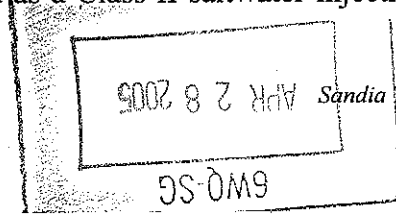
The Lyondell Chemical Company, Channelview Plant has safely disposed of over 1.0 billion gallons of process waste in the two waste disposal wells. Waste injection started in July 1978 into Plant Well 1 (WDW-148), with Plant Well 2 (WDW-162) being brought on line in January 1980. Both of the injection wells are cased-hole, perforated completions. Plant Well 1 (WDW-148) was perforated into Oligocene Frio sands Frio A, Frio B, and Frio C sands from 6,884 to 7,176 feet measured depth in the 1996 sidetrack well (Commingled Frio A/B/C Sand Injection Interval), and was perforated into the same sands in the original completion. In April 2004, this well was recompleted into the overlying Frio E&F Sand Injection Interval, with perforations from 6,690 feet to 6,818 feet. Plant Well 2 (WDW-162) was originally perforated into the Frio A/B/C Sand from 6,892 to 7,146 feet (measured depth). Plant Well 2 (WDW-162)



was recompleted into the Frio E&F Sand in April 2003 from 6,700 to 6,800 feet (measured depth) and currently injects into that injection interval.

Nearby offset Class I injection wells considered in the model include Merisol's Plant Well 1 (WDW-147) and Plant Well 2 (WDW-319), Equistar's Plant Well 1 (WDW-36), and Atofina's Plant Well 1 (WDW-122) and Plant Well 2 (WDW-230). Permitted maximum injection rates for these facilities as well as annotated injection well logs (1 log for each facility) are included in Appendix 2-6, Volume 3. Historic injection reports for these facilities are also included in Appendix 2-6, Volumes 9 through 12. Merisol's Plant Well 1 (WDW-147) is currently completed into the Frio E&F Sand and is currently limited to an injection rate of only 400 gpm. However, Merisol is also permitted to recomplete Plant Well 1 (WDW-147) into the underlying Frio A/B/C Sand Injection Interval (with the same rate limitation). Additionally, Merisol has a new well, Plant Well 2 (WDW-319), which was installed at the facility in September 2000, and is completed into the Frio A/B/C Sand Injection Interval. This well's permit allows for the same injection limitations in the injection interval sands as does Plant Well 1 (WDW-147). In the model, these two wells are modeled as a single point source, with the projected model period using an upper bound rate of 750 gpm in the Frio A/B/C Sand Injection Interval and the Frio E&F Sand Injection Interval. This rate limit is consistent with Merisol's 2000 HWDIR Exemption Petition Reissuance request currently being processed by EPA. Using this maximum injection rate of 750 gpm from the start of 2002 through year-end 2020 is conservative, since the facility is not as yet permitted or approved for this rate.

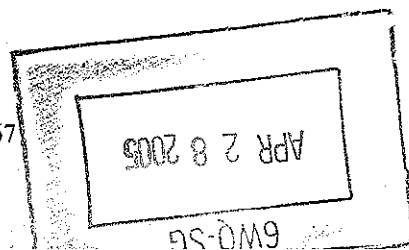
Equistar's Plant Well 1 (WDW-36) is currently completed in the Frio E, Frio F, and Frio A sands. Originally (1967 through 1977), the Equistar, Plant Well 1 (WDW-36) was completed in the Frio B Sand, the Frio C Sand. Although this well is limited to an injection rate of 350 gpm, the well is currently on standby and their waste stream is commingled with that disposed of in Lyondell Chemical Company's two wells. Plant Well 1 (WDW-36) has not been used on a sustained basis since 1980. The Frio A/B/C Sand Injection Interval models and the Frio E&F Sand Injection Interval models both consider historical and potential future injection into Equistar's Plant Well 1 (WDW-36). Atofina's Plant Well 1 (WDW-122) and Plant Well 2 (WDW-230) are completed in the Frio E and F through Frio C sands, although a parting in the protection casing of Plant Well 1 (WDW-122) allows some effluent to enter a permitted sand that overlies the Frio D Sand in that well. These two wells are limited to a maximum injection rate of 150 gpm, each. In the model, these two wells are modeled as a single point source. The Cobra Operating, Co., Texas Northern Railroad #6 well, located approximately 1.5 miles southeast of Plant Well 1 (WDW-148), is permitted as a Class II saltwater injection well. The



well is currently completed into the Frio C Sand (based on reported perforation depths and nearby wells with available logs) and has a maximum permitted rate of 29.2 gpm. Therefore, it is included in both model cases for the Frio A/B/ Sand Injection Interval modeling.

In the East Houston area, located along the south side of the Houston Ship Channel, there are several other industrial users of Class I injection wells. Well locations relative to the Lyondell Chemical Company Channelview Plant for these Class I injection wells are shown in Figure 2-1. Completion histories for the wells are shown in Table 2-15. These offset injection wells have been included in the Case 2 (Unsealed Fault Case) model, as further detailed in Section 2.5. Copies of the monthly injection rates, as reported to Texas Commission on Environmental Quality (TCEQ) for these facilities, are included in Appendix 2-6, Volumes 9 through 12. Completion and workover reports for these wells are included in Appendix 2-6, Volumes 6 through 9. An annotated well log from each facility is also included in Appendix 2-6, Volume 3. Figure 2-4 shows a southwest-northeast oriented structural-stratigraphic cross section through the Houston Ship Channel area Class I injection wells. Well completion intervals are annotated on each well, as well as their dates of completion. Figure 2-3 shows a northwest-southeast structural stratigraphic cross section extending from the Channelview Plant to the GNI Plant Well 1 (WDW-169). This schematic shows the juxtaposition of the lower Frio sands across the Renee-Lynchburg Field structure faults located between the Channelview Plant and the Houston Ship Channel injection well facilities. Note that the Houston Ship Channel injection well facilities are fault separated from the Lyondell Chemical Company Channelview Plant by several faults, one or more of which could be a barrier to fluid flow. Therefore, injection at these facilities is discounted in the Case 1 models, which conservatively assume that the closest fault (Fault A) is no flow boundary.

The Case 2 models conservatively assume that none of the Renee-Lynchburg faults are laterally sealing. Therefore, injection into these Houston Ship Channel area wells is included in this model case. Since these Houston Ship Channel area wells are or have been completed over multiple intervals, and since the cross-fault juxtaposition of sand-to-sand contacts across the Renee-Lynchburg Field faults sets up the possibility for cross-flow between multiple sand units, injection volume allocation in these wells is conservatively assigned at 100 percent to that unit being modeled. For example, in the case of the Case 2 - Frio E&F Sand Injection Interval models, all of the Houston Ship Channel well injection volumes are allocated fully to the Frio E&F Sand, even though several of the wells were partially or fully completed into deeper sand units.



For the Case 2 – Frio A/B/C Sand Injection Interval models, all of the Houston Ship Channel well injection volumes again are allocated fully to the modeled unit, even though several of the wells were partially or fully completed into shallower sands. Additionally, note that on Figure 2-4, the “Lower A&B Sand” (brown color sand) is correlative to the shale interval between the Frio A&B Sand and the Frio C Sand at the Channelview Plant. This sand is not present at the Lyondell Chemical Company facility wells. Potential injection into this Lower Frio A&B Sand (such as in the Shell injection wells – see Figure 2-4) is discounted, thereby increasing the modeled amount of pressure buildup in the Frio E&F Sand Injection Interval and the Frio A/B/C Sand Injection Interval.

The locations of the nearby facilities along the Houston Ship Channel are shown on Figure 2-1 and distances between the wells are tabulated in Table 2-16. Maximum permitted injection rates for these facilities are shown below.

Current Facility Name	Injection Well(s)	Maximum Rate(s)*
GNI	WDW-169 and WDW-249	500 gpm cumulative
Hampshire Chemical Corp.	WDW-222 and WDW-223	300 gpm cumulative
Shell	WDW-172 and WDW-173	Plugged
Vopak	WDW-157	300 gpm

* Rates from Texas Natural Resource Conservation Commission Underground Injection Control Database

Shell ceased injection into Plant Well 1 (WDW-172) in 1992, and ceased injection into Plant Well 2 (WDW-173) in 1995. Both wells have been plugged.

